

Recent Advance in 3D Object and Scene Generation: A Survey

XIANG TANG, Harbin Institute of Technology, Shenzhen, P.R.China

RUOTONG LI*, Pengcheng Laboratory, P.R.China

XIAOPENG FAN†, Harbin Institute of Technology, P.R.China

In recent years, the demand for 3D content has grown exponentially with intelligent upgrading of interactive media, extended reality (XR), and Metaverse industries. In order to overcome the limitation of traditional manual modeling approaches, such as labor-intensive workflows and prolonged production cycles, revolutionary advances have been achieved through the convergence of novel 3D representation paradigms and artificial intelligence generative technologies. In this survey, we conduct a systematically review of the cutting-edge achievements in static 3D object and scene generation, as well as establish a comprehensive technical framework through systematic categorization. Specifically, we initiate our analysis with mainstream 3D object representations, followed by in-depth exploration of two principal technical pathways in object generation: data-driven supervised learning methods and deep generative model-based approaches. Regarding scene generation, we focus on three dominant paradigms: layout-guided compositional synthesis, 2D prior-based scene generation, and rule-driven modeling. Finally, we critically examine persistent challenges in 3D generation and propose potential research directions for future investigation. This survey aims to provide readers with a structured understanding of state-of-the-art 3D generation technologies while inspiring researchers to undertake more exploration in this domain.

CCS Concepts: • **General and reference** → **Surveys and overviews**; • **Computing methodologies** → **Computer graphics**; **Computer vision**.

Additional Key Words and Phrases: 3D representation, 3D object generation, 3D scene generation, deep generative model

ACM Reference Format:

Xiang Tang, Ruotong Li, and Xiaopeng Fan. 2025. Recent Advance in 3D Object and Scene Generation: A Survey. *ACM Comput. Surv.* 1, 1 (April 2025), 34 pages. <https://doi.org/10.1145/nnnnnnnn.nnnnnnnn>

1 INTRODUCTION

Over the decades, automated content generation have been significant revolved. In the early years, rule-base modeling such as L-system [1] and procedural shape grammar [2, 3] showed their efficiency in creating objects and scenes with regular and repeat structures. Although it can generate 3D content with complex geometry and texture detail very fast, the rules and grammar are difficult manual designed until the neural networks and deep learning method revolutionizing computer vision in the 2010s. Guo et al. [4] employed deep learning to discover atomic structures, extracting rules from input images and converting them into L-systems to achieve inverse procedural

*Corresponding author

†Corresponding author

Authors' addresses: Xiang Tang, Harbin Institute of Technology, Shenzhen, Shenzhen, P.R.China, 24B951063@stu.hit.edu.cn; Ruotong Li, Pengcheng Laboratory, Shenzhen, P.R.China, lirt@pcl.ac.cn; Xiaopeng Fan, Harbin Institute of Technology, Harbin, P.R.China, fxp@hit.edu.cn.

Permission to make digital or hard copies of all or part of this work for personal or classroom use is granted without fee provided that copies are not made or distributed for profit or commercial advantage and that copies bear this notice and the full citation on the first page. Copyrights for components of this work owned by others than ACM must be honored. Abstracting with credit is permitted. To copy otherwise, or republish, to post on servers or to redistribute to lists, requires prior specific permission and/or a fee. Request permissions from permissions@acm.org.

© 2025 Association for Computing Machinery.

0360-0300/2025/4-ART \$15.00

<https://doi.org/10.1145/nnnnnnnn.nnnnnnnn>

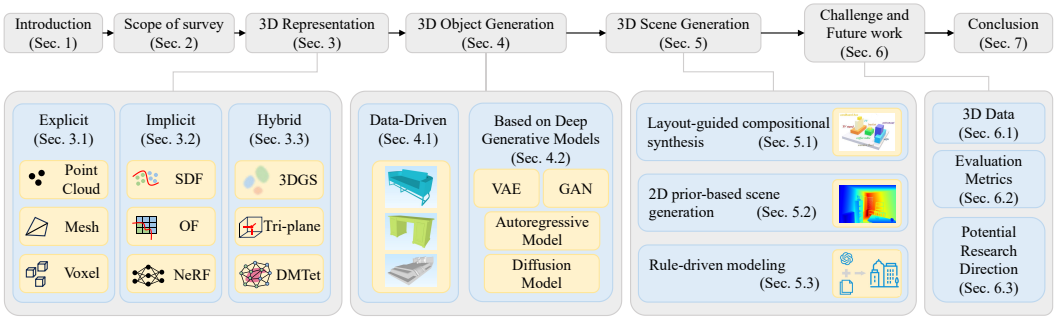


Fig. 1. Structure of this survey.

modeling. CropCraft [5] optimized plant morphological parameters through inverse procedural modeling to generate mesh representations of crops from images. With the breakthroughs in deep learning technologies, generative AI has made revolutionary progress in 2D content generation: text parsing and generation models represented by DeepSeek [6], text-to-image technologies led by Imagen [7] and GPT-4o [8], all demonstrate outstanding performance. Against the backdrop of rapid advancements in metadata, 3D content generation has gained widespread attention as a natural extension of 2D technology, yet its development faces multiple challenges. The increase in dimensionality complicates the effective integration of explicit 3D representations into neural network architectures. Simultaneously, novel rendering techniques based on implicit Neural Radiance Fields [9] struggle to directly adapt their generated content to traditional rasterized graphics pipelines. Furthermore, the scarcity of high-quality 3D asset datasets significantly makes model training more difficult.

Despite these limitations, significant progress has been achieved in 3D content generation, yielding several groundbreaking research outcomes. Among them, Point-E [10] constructs a million-scale 3D model-text paired dataset for training point cloud diffusion models, enabling text-to-3D point cloud generation. Several methods [11–18] incorporate 3D implicit representations into deep generative models and subsequently extract explicit meshes using algorithms [19, 20]. DreamFusion [21] introduced an innovative paradigm leveraging 2D generative priors to supervise 3D representation optimization, establishing new directions for subsequent research. Meanwhile, approaches such as [22–28] fully leverage the powerful text parsing capabilities of large language models (LLMs) to extract scene features from natural language descriptions for layout construction. RGBD2 [29] derives mesh representations of scenes from 2D image priors. The parametric generation framework proposed by Raistrick et al. [30] successfully achieved infinite combinatorial generation of natural resources based on mathematical rules. Therefore, this study is dedicated to systematically analyzing the related research in the field of 3D content generation, summarizing its technical paradigms and categorizing them accordingly. As shown in Table 1, we provide a structured overview of recent works, focusing on 3D representations, 3D object and scene generation methods.

As illustrated in Figure 1, this survey first delineates its scope and related works in Section 2. Section 3 introduces fundamental theories of 3D representations, analyzing their advantages, limitations, and integration with generative frameworks. Subsequently, we bifurcate 3D content generation into object-level and scene-level tasks. Section 4 introduces data-driven generative methods by leveraging publicly available datasets as an entry point. With the rapid development of deep generative models, researchers have extended these approaches to the 3D field, forming a unique generative paradigm. Expanding to scene generation in Section 5, we classify methodologies into three categories based on their theory: multi-object compositional synthesis guided by layouts or scene graphs, generation methods that directly extract scene representations from spatial information provided by 2D images, and rule-driven modeling with controllable details. The timeline

Table 1. Summary of representative works in 3D generation, classified by their generated "Content". The "GM" column indicates the adopted generative model, where "AR" denotes autoregressive models and "DM" represents diffusion models. The "3D Rep." column specifies the 3D representation format of generated objects. The "Opt." column describes the supervised optimization strategy employed. Additionally, we present each method's required input and whether it supports editability.

Methods	Content	GM	3D Rep.	Opt.	Input	Editability
DeepSDF [11]	Object Shape	VAE	SDF	3D	Uncon.	✗
SetVAE [31]	Object Shape	VAE	Point Cloud	3D	Uncon.	✗
AutoSDF [32]	Object Shape	AR	SDF	3D	Uncon./Text	✗
MeshXL [33]	Object Shape	AR	Mesh	3D	Uncon./Text/Image	✗
SurfGen [12]	Object Shape	GAN	SDF	3D	Uncon.	✗
GET3D [13]	Object	GAN	Tri-plane/DMTet	3D	Uncon./Text	✓
Barthel et al. [34]	Object	GAN	3DGS	3D	Uncon.	✓
DreamFusion [21]	Object	DM	NeRF	SDS	Text	✗
Yu et al. [35]	Object	DM	NeRF/DMTet	CSD	Text	✓
LucidDreamer [36]	Object	DM	3DGS	ISM	Text	✓
ProlificDreamer [37]	Object	DM	NeRF/DMTet	VSD	Text	✗
ScaleDreamer [38]	Object	DM	NeRF	ASD	Text	✗
DreamControl [39]	Object	DM	NeRF	SDS	Text	✗
Sculpt3D [40]	Object	DM	NeRF	2D&3D	Text	✗
Shap-E [41]	Object	DM	NeRF	3D	Text/Image	✗
MaPa [42]	Object Texture	DM	-	2D	Text/Image + Mesh	✓
TexGaussian [43]	Object Texture	DM	3DGS	3D	Uncon./Text	✗
InstructScene [44]	Indoor Scene	DM	Mesh/Point Cloud	3D	Text	✗
MMGDreamer [45]	Indoor Scene	DM	SDF	3D	Text/Image	✗
SceneCraft [46]	Indoor Scene	DM	NeRF	2D	Text	✗
GenRC [47]	Indoor Scene	DM	Mesh	2D	Text/Image	✗
DreamScene [25]	Cross-Scene	DM	3DGS	CSD	Text	✓
WonderWorld [48]	Cross-Scene	DM	3DGS	2D	Text	✗
3D-GPT [27]	Outdoor Scene	-	Mesh	-	-	✓
Proc-GS [49]	Outdoor Scene	-	3DGS	-	Text/Image	✓

diagrams for these representative works can be found in Appendix Figures 5 and 6 respectively. Lastly, Section 6 identifies remaining challenges in the field and outlines potential future research directions. We aim to provide technical references for researchers and inspire subsequent works through this review.

Our principal contributions can be summarized as follows:

- We propose a novel taxonomy by decomposing 3D content generation into object and scene generation, systematically summarizing and categorizing their technical routes respectively.
- This review comprehensively covers extensive literature spanning the past five years, emphasizing integration of the latest breakthroughs to comprehensively present technological development trajectories and cutting-edge dynamics.

2 SCOPE OF THIS SURVEY

This survey highlights recent advancements in 3D generation techniques for static object and scene generation tasks. Our focus lies on systematically categorizing and summarizing 3D generation paradigms and their application scenarios. The primary scope covers seminal papers published in top-tier computer vision and computer graphics conferences/journals from 2020 to 2025, supplemented by pre-prints from arXiv recently. Instead of exhaustive technical analysis, we curate

representative studies to distill their core methodological frameworks, enabling readers to efficiently grasp technical trajectories and construct structured knowledge graphs. It should be noted that this survey explicitly excludes dynamic 3D content and human-related generation methods (e.g., avatar modeling, full-body reconstruction, and motion synthesis).

In contrast to [50], our work focuses on 3D content generation techniques rather than conducting compatibility analysis between 3D representations and generative models. Unlike previous surveys that focus on text-to-3D generation [51, 52], this survey comprehensively covers also the image-driven generation and unconditional 3D generation. For extended discussions on uni-modal and multi-modal generation (e.g., image, video, 3D, and audio), readers may refer to [53]. Notably, as a valuable supplement to existing 3D content generation surveys [54, 55], this is the first review to holistically cover complete technical pathways for 3D object and scene generation, while proposing novel insights into methodological evolution and application expansion.

3 3D REPRESENTATIONS

In the field of 3D content generation, the choice of 3D model representation not only influences the generative method chosen but also affects the quality and efficiency of the generation algorithms. In this section, we go through 3D representations and categorize them based on mathematical expressions and geometric description mechanisms: explicit representation, implicit representation, and hybrid representation.

3.1 Explicit Representations

Typical explicit representations include meshes, point clouds and voxels. This representation directly describes the spatial structure of 3D objects through discrete geometric elements. It supports geometric editing and precise control of geometry details and is widely used in traditional computer graphics tasks such as modeling, rendering, and simulation.

3.1.1 Mesh. Polygonal mesh representation, as a fundamental paradigm for 3D geometric modeling, defines geometric shapes by explicitly encoding the 3D coordinates of vertices and their topological adjacency relationships, enabling compact and precise geometric descriptions. Thanks to its explicit parameterization, mesh models support efficient rendering operations and affine transformations (including translation, rotation, scaling, etc.). As an early attempt to generate object meshes, Pixel2Mesh [56] employed graph convolutional networks (GCN) to process meshes by defining model vertices and edges as nodes and connections in the graph, directly generating 3D meshes from single images. Gkioxari et al. [57] leveraged GCN to iteratively optimize mesh vertex positions initialized from voxels. By fusing image features through vertex alignment, they enhanced detail accuracy and constructed a system to achieve joint 2D detection and 3D mesh extraction from real-world images.

3.1.2 Point clouds. Point clouds consist of unordered discrete sampling points distributed in three-dimensional Euclidean space, where each point is parameterized by Cartesian coordinates (x, y, z) and may be extended with additional attributes such as RGB values, surface normals, reflectivity, etc. The data acquisition primarily relies on structured light scanning, LiDAR, or Time-of-Flight (ToF) depth sensing technologies, which directly capture the spatial sampling distribution of target object surfaces. In the realm of 3D generation, Sun et al. [58] proposed a point-wise generation approach to construct point clouds, enabling visualization and interpretability during the generation process. Kim et al. [31] leveraged permutation-invariant attention modules to process unordered 3D point sets. The recent work by Nichol et al. [10] introduced a point cloud diffusion model to achieve text-to-3D point cloud generation.

3.1.3 Voxel. Voxels are essentially topological extensions of 2D pixels in the 3D. By dividing the Euclidean space into a uniform 3D grid array, each cubic unit, i.e. voxel, is assigned a specific attribute value (such as density, color, material properties or scalar field information) to encode the spatial occupancy state and physical properties. This structured representation exhibits strictly isotropic spatial distribution characteristics, providing an ideal input structure for volume data feature extraction based on 3D convolutional neural networks. Representative works, such as Clip-Forge [59], encode voxels into latent vectors through 3D convolutions, which are subsequently reconstructed by a decoder. The shape embeddings are then mapped to a Gaussian distribution to support the generation of diverse shapes. Wu et al. [60] employ a fully convolutional network with progressive upsampling to map latent vectors to 3D voxels. Notably, as the spatial resolution increases, the complexity of storing voxels grows at an $O(n^3)$ rate, leading to dual constraints of memory and computational power during high-precision modeling.

3.2 Implicit Representations

Implicit representations implicitly encode the geometric and radiation characteristics of three-dimensional space through continuous mathematical functions $\mathcal{F} : \mathbb{R}^3 \rightarrow \mathbb{R}^k$, where the output dimension k corresponds to multimodal features such as signed distance, occupancy probability or radiation properties. This continuous representation paradigm naturally supports differential operations, making differentiable rendering based on volume rendering equations possible.

3.2.1 Signed Distance Function. The Signed Distance Function (SDF) is defined as the directed distance $\phi(\mathbf{x})$ from any point \mathbf{x} to the target surface, constructing a zero-level set surface representation that satisfies $\{\mathbf{x} | \phi(\mathbf{x}) = 0\}$. The sign property of this function (negative values inside and positive values outside) not only provides a topological basis for distinguishing the interior-exterior relationship of the geometry, but its global continuity and potential differentiability also endow it with unique advantages in mathematical processing. 3D generation methods, such as SDFusion [61], encode SDF into latent vectors for model training, and use a decoder to recover the SDF shape representation of objects from sampled noise during inference. One-2-3-45 [62] and One-2-3-45++ [63] leverage neural networks to predict SDF values on object surfaces, followed by high-fidelity mesh conversion through isosurface extraction algorithms such as Marching Cubes [19].

3.2.2 Occupancy Field. By defining the occupancy probability function $o(\mathbf{x}) \in [0, 1]$ for spatial points \mathbf{x} , Occupancy Field transforms geometric surface reconstruction into a 3D binary classification problem. Mescheder et al. [64] employ deep neural networks to parameterize occupancy field, leveraging the Marching Cubes algorithm [19] to extract explicit meshes at the isosurface where $o(\mathbf{x}) = 0.5$. Compared with SDF, occupancy field replaces signed distance regression with probabilistic supervision, significantly reducing optimization complexity while demonstrating superior generalization capabilities for high-genus topologies or non-closed surfaces. However, this approach faces inherent limitations: surface localization accuracy is constrained by spatial sampling resolution, and the absence of signed distance information leads to insufficient smoothness in reconstructed surfaces.

3.2.3 Neural Radiance Fields. Neural Radiance Fields (NeRF) [9] has attracted widespread attention since its introduction. This method models static scenes as a mapping function $F_{\Theta} : (\mathbf{x}, \mathbf{d}) \mapsto (\sigma, \mathbf{c})$ that maps spatial coordinates \mathbf{x} and viewing directions \mathbf{d} to volume density σ and view-dependent radiance \mathbf{c} , with a Multi-Layer Perceptron (MLP) serving as the function approximator. The core innovation lies in the introduction of a high-frequency positional encoding function, which enhances the MLP's geometric detail representation capabilities through Fourier feature expansion. Based on volume rendering theory, pixel color computation along a camera ray $\mathbf{r}(t) = \mathbf{o} + t\mathbf{d}$ can be

discretized as:

$$C(\mathbf{r}) = \sum_{i=1}^N T_i (1 - \exp(-\sigma_i \delta_i)) \mathbf{c}_i, \quad \text{where } T_i = \exp\left(-\sum_{j=1}^{i-1} \sigma_j \delta_j\right) \quad (1)$$

where δ_i denotes the sampling interval and T_i represents the cumulative transmittance. Although NeRF achieves photorealistic novel view synthesis, its per-ray integration strategy results in significant rendering latency. Subsequent works such as Instant-NGP [65] utilize multiresolution hash encoding for accelerated training. Meanwhile, DreamFusion [21] introduced the NeRF representation into the realm of 3D generation, inspiring a series of research.

3.3 Hybrid Representations

In order to combine the advantages of explicit and implicit representations, emerging research tends to build a hybrid representation framework. This method breaks through the inherent limitations of a single representation and dynamically combines explicit geometric primitives and implicit field functions at different spatial scales, levels of detail or functional modules to form a hierarchical scene description system.

3.3.1 3D Gaussian Splatting. The 3D Gaussian ellipsoids are initialized using sparse point clouds generated by Structure-from-Motion (SfM) [66]. Their parametric representation encompasses attributes including center positions, covariance matrices, colors, and opacities. Through a differentiable optimization process, this approach models 3D objects as collections of anisotropic Gaussian distributions. "Splatting" refers to the process of projecting ellipsoids onto the image plane. 3D Gaussian Splatting (3DGS) [67], by virtue of the geometric editability enabled by explicit primitives, high-frequency detail capture capability comparable to implicit radiance fields, and real-time rendering efficiency, has been widely applied in 3D generation tasks [68–70]. However, its storage complexity grows linearly with the number of Gaussian ellipsoids, and the generation quality heavily depends on point cloud priors.

3.3.2 Tri-plane. The Tri-plane representation, originally proposed by EG3D [71], decomposes 3D spatial features into three orthogonal Cartesian planes (XY, XZ, YZ). For any 3D point \mathbf{x} , its corresponding feature vectors F_{xy} , F_{xz} , and F_{yz} are projected onto these planes and combined via simple weighted aggregation to generate the final 3D feature vector \mathbf{F} . A MLP then maps \mathbf{F} to point attributes such as color and density. Specifically, EG3D [71] innovatively integrates the tri-plane architecture with the StyleGAN2 [72] framework, leveraging generative adversarial networks (GANs) to directly synthesize tri-plane features and combining them with differentiable volume rendering for high-fidelity 3D face generation. TensorRF [73] employs tensor decomposition to decouple the 3D feature field into a product of planar matrices and vector modes, reducing storage complexity from $O(n^3)$ to $O(n^2)$ while maintaining reconstruction quality.

3.3.3 DM Tet. As a groundbreaking framework for hybrid 3D representation, DM Tet [74] discretizes the 3D space into structured deformable tetrahedral meshes, where each vertex is associated with implicit SDF values and their gradient information. By leveraging neural networks for collaborative optimization, it dynamically extracts explicit surface meshes through the differentiable Marching Tetrahedra algorithm [20], enabling efficient and high-precision geometric modeling. The key advantages of DM Tet lie in its capability to handle complex 3D geometric structures and surface details, as well as its seamless integration with differentiable rendering methods. In 3D object generation approaches, both Magic3D [15] and Magic123 [16] adopt a two-stage optimization framework, converting the implicit NeRF representations from the initial stage into DM Tet for further refinement. The latest work Sherpa3D [18] ensures multi-view consistency of generated

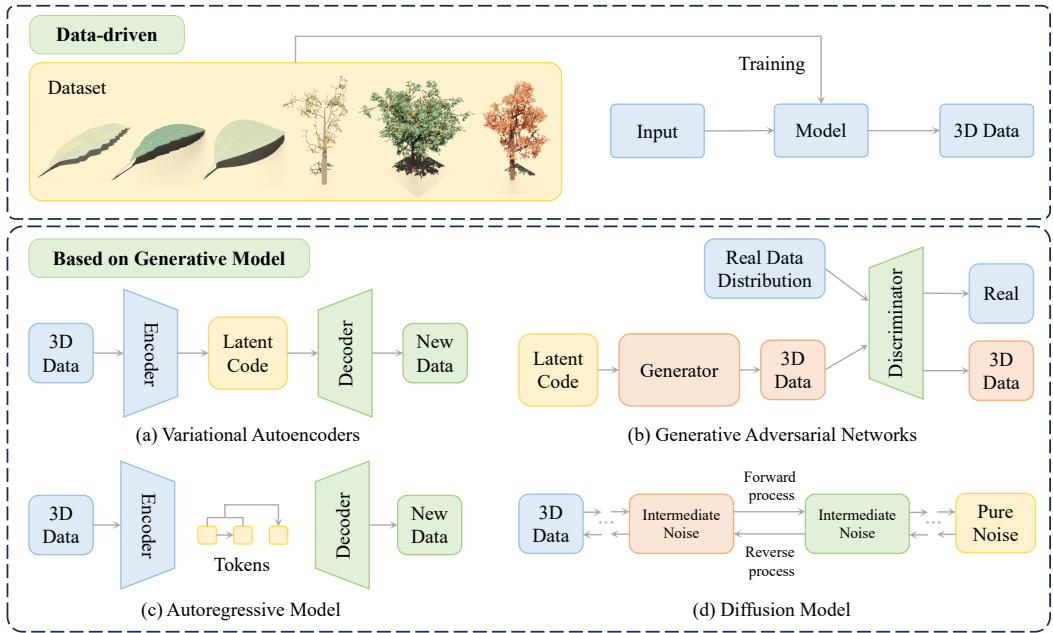


Fig. 2. Two major paradigms of 3D object generation methods.

objects by optimizing coarse 3D object priors represented through DM Tet, which are produced by the 3D diffusion model (i.e., Shap-E [41]).

4 3D OBJECT GENERATION

As illustrated in Figure 2, the 3D object generation technology primarily follows two research paradigms. The first category employs data-driven approaches, which train models using large-scale datasets and utilize feedforward inference mechanisms to achieve efficient generation of 3D assets. The second paradigm focuses on integrating deep generative frameworks with diverse 3D representations to construct generalized 3D generation systems that support both unconditional and conditional generation.

4.1 Data-driven

Data-driven 3D content generation methods achieve efficient inference by establishing mapping relationships between input data and 3D representations, with their performance critically dependent on the scale and quality of training data. However, constructing large-scale 3D asset datasets faces multifaceted challenges. Compared to 2D images, 3D data acquisition requires specialized equipment (e.g., LiDAR, depth cameras) or professional modeling software, resulting in exponentially higher collection costs. Furthermore, existing public 3D datasets commonly suffer from limited object category coverage and low geometric complexity. These constraints directly lead to the relative limitation of data-driven paradigms in 3D generation research. As summarized in Table 2, current mainstream datasets for 3D generation tasks can be categorized into three types based on data modalities: 3D model datasets, 2D image/video datasets, and 3D model-text paired datasets.

In terms of model-text paired data, Text2Shape [123] pioneered semantic alignment between natural language texts and 3D shapes through joint embedding learning. Their dataset constructed from a ShapeNet subset [80] with corresponding textual descriptions validated the feasibility of this approach. Building on this work, ShapeCraft [124] extended the dataset to create Text2Shape++,

Table 2. Classify the common datasets according to the data types. We have documented the size of each dataset and the number of object categories it contains, which are connected by the symbol "-". In addition, the "Application" column indicates whether the dataset is used for training, testing, or validation in the corresponding generation method.

Datasets	Data type	Size	Categories	Application
GSO [75]	3D Model	1K	17-Household Items	[62, 76-79]
ShapeNetCore [80]	3D Model	51K	55 - Objects	[11, 13, 31-33, 43, 58-61, 81-88]
ModelNet [89]	3D Model	127K	662 - Objects	[58, 60]
PartNet [90]	3D Model	26.6	24 - Objects	[86, 87]
Objaverse [91]	3D Model	800K	Objects	[33, 43, 62, 63, 77-79, 81, 88, 92-101]
Objaverse-XL [102]	3D Model	10.2M	Objects	[33, 103]
3D-Future [104]	3D Model + RGB Image	16.5K(Models) + 20.2K(Images)	34 - Furniture + Indoor scenes	[22, 33, 45, 103, 105-107]
3D-Front [108]	RGB Image	6.8K(Houses) + 51.7K(Rooms)	28 - Indoor Scenes	[22, 44, 105-107, 109-114]
MVImgNet [115]	RGB Image	6.5M	238 - Objects	[77]
ScanNet [116]	RGBD Image	2.5M	Indoor Scenes	[22, 29, 36, 47, 117]
HyperSim [118]	RGBD Image	77.4K	461 - Indoor Scene	[46, 119]
CO3D [120]	Video	19K	50 - Objects	[121]
uCO3D [122]	Video	170K	1000 - Objects	-
Text2Shape [123]	3D Model - Text pairs	15K(Models) + 75K(Text)	2 - Objects	[123]
Text2Shape++ [124]	3D Model - Text pairs	369K	Objects	[124]
Point-E [10]	3D Model - Text pairs	>1M(Models) + 120K(Text)	Objects	[10], [41]

containing 369K high-quality model-text pairs to support recursive text-conditioned 3D shape generation. The OpenAI team proposed Point-E [10], which built a million-scale 3D asset dataset with linguistic descriptions for training point cloud diffusion models, creating a text-to-image-to-point cloud generation pipeline, though the dataset remains non-public. Its successor Shap-E [41] adopted a similar 3D dataset and extended it by innovatively mapping point clouds and rendered views into implicit function parameters using encoders. By training latent diffusion models on encoder-derived latent vector sequences, this approach generates 3D representations through denoising processes under text/image conditions, demonstrating superior convergence speed and generation quality compared to Point-E [10]. In particular, limited text-3D data pairs restrict the vocabulary coverage of generative models and fine-grained control over text conditions, often resulting in stereotypical outputs for specific prompts and diminished open-vocabulary generation capability. To address this issue, TextField3D [81] proposed injecting dynamic noise into text embeddings to map limited 3D data into broader text latent spaces for better alignment.

The emergence of Contrastive Language-Image Pre-training (CLIP) [125] provides novel insights for addressing the scarcity of 3D assets. Pre-trained on massive image-text pairs, CLIP learns a joint visual-linguistic representation space through feature similarity computation between encoded images and texts. This powerful cross-modal alignment capability has inspired numerous generation methods that bypass the need for 3D-text paired data. CLIP-Forge [59] integrates CLIP with conditional normalizing flows to directly learn text-to-rendered image-to-3D shape correlations, constructing a zero-shot 3D generation framework. CLIP-Sculptor [82] trained two independent vector-quantized variational autoencoders (VQVAEs) to encode object voxel grids at different resolutions into latent codes, followed by training coarse and fine-grained Transformers to generate low and high-resolution latent grids conditioned on CLIP image embeddings. During inference, natural language is converted into embeddings using CLIP text encoders, which pass through the Transformers to decode latent codes into high-fidelity 3D shapes. Expanding beyond shape generation, CLIP-NeRF [126] and CLIP-Mesh [127] incorporate texture modeling. Specifically, the former decouples NeRF's shape and appearance controls into two independent latent codes and trains feedforward networks to convert CLIP embeddings into latent code offsets for 3D shape and texture editing. The latter utilizes pre-trained CLIP models and differentiable renderers to optimize 3D mesh control vertices, textures, and normal maps for text-aligned 3D asset generation. Text2Mesh [128] focuses on leveraging CLIP's cross-modal alignment capabilities to optimize colors and enhance geometric details of low-quality meshes. Dream3D [83] first generates stylized views

	Training Stability	Generation Quality	Probabilistic Interpretation	Inference Speed	Generation Diversity	Application Scenarios	Usage Frequency in 3D Generation
VAE	✓✓✓	✓	✓✓✓	✓✓✓	✓✓	Image Generation, Data Compression	✓✓
GAN	✓	✓✓✓	✓	✓✓✓	✓✓✓	Image Generation, Style transfer	✓✓
Autoregressive Model	✓✓✓	✓✓	✓✓✓	✓✓	✓✓	Text/Image/Audio Generation	✓
Diffusion Model	✓✓✓	✓✓✓	✓✓✓	✓	✓✓✓	Image/Audio Generation	✓✓✓

Fig. 3. Qualitative comparison of deep generative models across different dimensions. The more symbols ✓ there are, the better the performance.

as geometric priors using text-to-image diffusion models (i.e., Stable Diffusion[129]), then combines CLIP guidance for high-quality 3D content generation, significantly improving geometric accuracy and visual quality under zero-shot conditions. Ge et al. [130] constructed a dataset to train CLIP for aligning images with LEGO models, combined with decal generation and UV printing, thereby enabling the creation of LEGO figurine from a single image.

4.2 Based on Generative Models

In recent years, deep generative models have achieved transformative breakthroughs in 2D image generation, leveraging their sophisticated representation learning capabilities. Prominent architectures such as Generative Adversarial Networks (GANs), Variational Autoencoders (VAEs), autoregressive models, and diffusion models have demonstrated unprecedented capacities in modeling intricate visual distributions. Based on the core characteristics of the aforementioned architectures, Figure 3 presents a qualitative comparison of them from dimensions such as performance and probabilistic interpretability. Motivated by these advancements, an increasing number of studies have focused on integrating such generative frameworks with diverse 3D representations to expand their applicability into the domain of 3D object generation. In this section, we systematically expounds on the foundational theoretical frameworks of generative models and provides an in-depth exploration of their innovative applications in 3D object generation methodologies.

4.2.1 Variational Autoencoders.

Variational Autoencoders (VAEs) [131] achieve probabilistic latent representation learning of data through an encoder-decoder architecture. The encoder maps input data to probability distribution parameters in the latent space via nonlinear transformations, with the reparameterization trick enabling sampling from this distribution to generate statistically diverse latent codes. The decoder, typically symmetric to the encoder, reconstructs latent codes into input-space data, forming an end-to-end generative system. The model optimizes the generative distribution by maximizing the evidence lower bound (ELBO), thereby achieving probabilistic modeling of data distributions.

VAEs exhibit significant advantages in explicit probabilistic modeling and stable training, yet they are confronted with limitations in generating high-quality outputs. In the domain of 3D object generation, DeepSDF [11] pioneered the integration of SDF with VAEs, enabling precise reconstruction of 3D object surfaces through differentiable Marching Cubes algorithm [19]. SetVAE [31] further introduces hierarchical variational autoencoders and attention mechanisms, achieving high-fidelity 3D shape generation using point cloud representations. Recent research directions have increasingly focused on hybrid architectures combining VAEs with other generative frameworks.

Specifically, TM-NET [132] represents a notable advancement by implementing joint encoding of part-level geometry and texture, which is then coupled with conditional autoregressive models to generate high-quality textured meshes. SDFusion [61], Michelangelo [84] and 3DTopia-XL [92] have demonstrated innovative approaches by integrating VAEs with diffusion models. The latest work, Trellis [103], defines a unified structured latent representation for 3D assets, training a sparse VAE on approximately 500K high-quality 3D assets carefully curated from four public datasets to learn structured latent representations. During the generation phase, the obtained latent representations of objects are decoded into 3DGS/radiance field/mesh representations. These frameworks not only generate semantically consistent 3D objects but also support conditional generation guided by textual or visual inputs, thereby expanding the applicability of VAE-based methods in interactive 3D object generation.

4.2.2 Generative Adversarial Networks.

Generative Adversarial Networks (GANs) [133] is a deep generative model based on adversarial training, which has achieved remarkable results in image generation tasks. The core idea of GANs is to construct a zero-sum game between the generator G and the discriminator D ; G tries to generate samples to steal D , while D strives to distinguish real data from data. This competition eventually converges to a generative Nash equilibrium, making the generated data samples close to the real distribution. The optimization goal of GAN can be formalized as the following minimax problem:

$$\min_G \max_D V(D, G) = \mathbb{E}_{x \sim p_{\text{data}}} [\log D(x)] + \mathbb{E}_{z \sim p_z} [\log(1 - D(G(z)))] \quad (2)$$

where z is the latent space noise input, p_{data} is the real data distribution, and p_z is the noise distribution. During the training process, one side is fixed and iterates alternately.

Building upon the groundbreaking advancements of GANs in 2D image generation, researchers have actively explored their potential in 3D content generation tasks in recent years. In early studies, Wu et al. [60] pioneered the extension of 2D convolutions to 3D voxel space, generating object shapes through adversarial training. This framework was further enhanced through the 3D-VAE-GAN architecture, which introduced an encoder to map 2D images into latent vectors for conditional generation. Similarly combining GANs with VAE, SurfGen [12] employed DeepSDF [11] as the generator to extract 3D surface meshes. It then transformed irregular 3D meshes into regular spherical parameterizations and leveraged GCN to extract features from spherical projections. By designing adversarial loss functions based on surface geometric features, this approach directly optimized object surfaces through adversarial training, effectively addressing the insufficient geometric constraints in traditional methods.

To fully exploit 2D visual priors for guiding 3D generation, 3D-aware GANs have emerged. These methods focus on constructing implicit or explicit 3D representations through generators, followed by differentiable rendering to synthesize 2D images. The discriminator then evaluates discrepancies between generated and real images to optimize the generation process. Specifically, HoloGAN [134] became the first unsupervised generative model to learn 3D representations from unlabeled 2D images. It utilized 3D convolutional networks to generate 3D features from fixed tensors, applied rigid transformations to enable arbitrary pose adjustments, and finally projected 3D features into 2D feature maps via differentiable perspective projection for image generation. Similarly, BlockGAN [135] disentangled 3D objects from scenes by employing separate generators to produce pose-adjustable 3D features, and merged multiple object features into unified scene features. Henzler et al. [136] extracted 3D voxels from 2D images, incorporated differentiable rendering layers for image synthesis, and optimized 3D structures using GAN loss. GET3D [13] introduced a DM Tet-based geometric representation coupled with tri-plane texture mapping, achieving high-fidelity 3D textured mesh generation through adversarial training. While NeRF-based geometry-aware

GANs (e.g., EG3D[71]) enable multi-view consistent geometry generation, their rendering efficiency remains a bottleneck. Notably, Barthel et al. [34] recently proposed an innovative approach that employs sequential decoders to translate tri-plane features into Gaussian attributes. By fine-tuning backbone networks, their method achieves end-to-end conversion from pretrained 3D-aware GANs' implicit neural radiance fields to 3D Gaussian splatting representations.

4.2.3 Autoregressive Models.

Autoregressive models are modeled by decomposing the joint distribution of high-dimensional data into a product of conditional distributions. Formally, given a sequence of variables $\mathbf{x} = (x_1, x_2, \dots, x_T)$, the joint probability $p(\mathbf{x})$ is expressed as:

$$p(\mathbf{x}) = \prod_{t=1}^T p(x_t | x_{<t}) \quad (3)$$

where each element x_t is generated conditioned on all preceding elements $x_{<t}$. This sequential dependency enables autoregressive models to capture complex local and global patterns in data.

The autoregressive framework, initially achieving remarkable success in image generation (e.g., PixelRNN [137]) and natural language processing (e.g., GPT [138]), has been progressively adapted to 3D generation tasks due to its inherent capability to model structural and sequential dependencies in 3D data. The self-attention mechanism of the Transformer [139], which enables efficient long-range dependency modeling, is widely adopted as the backbone architecture for autoregressive models. Early attempts such as PointGrow [58] employed autoregressive strategies for point-wise cloud generation, leveraging self-attention to capture long-range dependencies while decomposing generation into interpretable per-point decisions. However, this approach exhibited suboptimal performance in handling large-scale point sets and shape completion tasks. PolyGen [85] and MeshXL [33] adopted a mesh-based generation paradigm. Specifically, PolyGen decomposed the generation of vertices and faces into sequential prediction problems, used the n -gon representation to improve efficiency, and extended the generalization ability through data augmentation and conditional generation. MeshXL proposed the Neural Coordinate Field (NeurCF), which encodes coordinate points into implicit neural embeddings to obtain face and mesh embeddings sequentially. It uses a predefined ordering strategy to convert unstructured meshes into ordered sequences and then directly generates high-fidelity 3D meshes through an autoregressive Transformer model. AutoSDF [32] compresses SDF into a low-dimensional discrete latent codes via VQVAE, ensuring local feature independence through patch-wise encoding. Its Transformer architecture learns the distribution of the discrete latent space and breaks the sequential dependence through a randomly arranged sampling order, enabling conditional generation at any spatial location. ShapeFormer [86] represents shapes through sparse local feature sequences and vector quantization compression, which supports efficient Transformer modeling. It can generate multiple reasonable 3D shape completion results from partial or noisy point clouds. Notably, these autoregressive methods focus exclusively on object geometric generation while neglecting texture synthesis, resulting in significant limitations for holistic 3D content creation.

4.2.4 Diffusion Models.

Most diffusion models currently adopted are based on DDPM [140], whose theoretical framework traces back to the diffusion probabilistic model proposed in [141]. Diffusion models consist of two processes: the forward process and the reverse process. In the forward diffusion process, data x_0 is gradually transformed into pure noise x_T via a fixed Markov chain, with Gaussian noise of

increasing variance added at each step:

$$\begin{aligned}
 q(x_t|x_{t-1}) &= \mathcal{N}(x_t; \sqrt{1 - \beta_t}x_{t-1}, \beta_t\mathbf{I}) \\
 q(x_{1:T}|x_0) &= \prod_{t=1}^T q(x_t|x_{t-1})
 \end{aligned} \tag{4}$$

where β_t denotes the variance at timestep t , with $0 < \beta_1 < \dots < \beta_T < 1$ controlling the noise schedule. The reverse process aims to denoise the data, where the diffusion model learns a neural network $p_\theta(x_{t-1}|x_t)$ to approximate the true reverse transition $q(x_{t-1}|x_t)$:

$$\begin{aligned}
 p_\theta(x_{t-1}|x_t) &= \mathcal{N}(x_{t-1}; \mu_\theta(x_t, t), \Sigma_\theta(x_t, t)) \\
 p_\theta(x_{0:T}) &= p(x_T) \prod_{t=1}^T p_\theta(x_{t-1}|x_t)
 \end{aligned} \tag{5}$$

with $p(x_T) = \mathcal{N}(x_T; 0, \mathbf{I})$. The model is optimized by minimizing the variational lower bound, which simplifies to:

$$\mathcal{L}_{\text{simple}} = \mathbb{E}_{t, x_0, \epsilon} [\|\epsilon - \epsilon_\theta(x_t, t)\|^2] \tag{6}$$

Methods based on other generative architectures are primarily limited to modeling object geometry and often suffer from a lack of texture detail. In contrast, approaches that lift diffusion models specialized in 2D image generation to 3D domain not only enable high-precision geometric reconstruction of objects but also produce textures with rich details. Early work, Zhou et al. [87] proposed a framework combining point-voxel representations with diffusion models for 3D shape generation and completion. In the domain of text-to-3D, DreamFusion [21] pioneered the use of pre-trained 2D diffusion models to guide text-to-3D object generation, introducing the groundbreaking concept of Score Distillation Sampling (SDS). Specifically, considering a differentiable 3D representation parameterized by θ and a rendering function g . For a given camera pose c , the rendered image can be expressed as $x = g(\theta, c)$. SDS optimizes the 3D representation parameters θ using a fixed-parameter 2D diffusion model ϕ . The core idea lies in adjusting θ by computing specific gradients to align the rendered image x with the distribution of the 2D text-to-image model. The specific gradient calculation formula is defined as:

$$\nabla_\theta \mathcal{L}_{\text{SDS}}(\phi, x = g(\theta, c)) = \mathbb{E}_{t, \epsilon, c} \left[w(t) (\hat{\epsilon}_\phi(x_t; y, t) - \epsilon) \frac{\partial x}{\partial \theta} \right] \tag{7}$$

where $\mathbb{E}_{t, \epsilon, c}$ denotes the expectation over timestep t , noise ϵ , and camera pose c ; $w(t)$ is a time-dependent weighting function that adjusts the importance of information at different timesteps; $\hat{\epsilon}_\phi(x_t; y, t)$ represents the noise predicted by the 2D diffusion model ϕ at timestep t under text prompt y ; ϵ is the ground-truth noise added to the rendered image x ; and $\frac{\partial x}{\partial \theta}$ is the gradient of the rendering function g with respect to parameters θ , quantifying the impact of parameter changes on the rendered image. Through iteratively computing gradients and updating θ , the rendered image progressively aligns with the distribution of images generated by the 2D text-to-image model, thereby optimizing the 3D representation.

SDS-based Approaches. This groundbreaking approach laid a theoretical foundation for subsequent 3D generation research based on pre-trained models. Numerous follow-up studies [14, 15, 18, 68, 69, 78, 93, 96, 121, 142] have also adopted SDS to optimize 3D representations. Similar to DreamFusion, RealFusion [121] optimizes NeRF to represent objects, achieving full 360° reconstruction of objects from a single image. Make-it-3D [142] leverages diffusion priors, reference view supervision, and depth priors to optimize NeRF for obtaining a coarse model, which is then converted into a textured point cloud for further refinement. Compared to NeRF-based

Table 3. The gradient calculation formula of the state-of-the-art score distillation methods. Additionally, using Instant-NGP [65] as the 3D representation, we conduct a quantitative comparison of different score distillation methods under specific prompts. The evaluation metrics include "Sim," which indicates the semantic similarity between generated images and the text, and "R@1," representing the CLIP recall rate. This metric measures the classification accuracy of predicting the correct text prompt by applying the CLIP model to rendered images.

Methods	Gradient Calculation Formula	Notation Explanation	Sim \uparrow	R@1 \uparrow
SDS [21]	$\mathbb{E}_{t,\epsilon,c} \left[w(t) (\hat{\epsilon}_\phi(x_t; y, t) - \epsilon) \frac{\partial x}{\partial \theta} \right]$	Section 4.2.4	0.288	1.000
ISM [143]	$\mathbb{E}_{t,\epsilon,c} \left[w(t) (\hat{\epsilon}_\phi(x_t; y, t) - \hat{\epsilon}_\phi(x_s; \emptyset, s)) \frac{\partial x}{\partial \theta} \right]$	$\hat{\epsilon}_\phi(x_s; \emptyset, s)$: The noise estimate at timestep s without a text prompt y .	-	-
CSD [35]	$\mathbb{E}_{t,\epsilon,c} \left[w(t) (\hat{\epsilon}_\phi(x_t; y, t) - \hat{\epsilon}_\phi(x_t; \emptyset, t)) \frac{\partial x}{\partial \theta} \right]$	$\hat{\epsilon}_\phi(x_t; \emptyset, t)$: The noise estimate at timestep t without a text prompt y .	0.280	0.936
VSD [37]	$\mathbb{E}_{t,\epsilon,c} \left[w(t) (\hat{\epsilon}_\phi(x_t; y, t) - \epsilon_{\phi'}(x_t; y, t, c)) \frac{\partial x}{\partial \theta} \right]$	$\epsilon_{\phi'}(x_t; y, t, c)$: The noise estimate predicted by a LoRA-fine-tuned model.	0.276	0.932
ASD [38]	$\mathbb{E}_{t,\epsilon,c} \left[w(t) (\hat{\epsilon}_\phi(x_t; y, t) - \hat{\epsilon}_\phi(x_{t+\Delta t}; y, t + \Delta t)) \frac{\partial x}{\partial \theta} \right]$	$\hat{\epsilon}_\phi(x_{t+\Delta t}; y, t + \Delta t)$: The noise estimate at a timestep $t + \Delta t$ with a text prompt y .	0.289	1.000

approaches, methods employing 3DGS for object modeling exhibit significantly faster convergence. DreamGaussian [68] introduces an efficient algorithm to convert generated Gaussians into textured meshes. GaussianDreamer [69] utilizes 3D diffusion models (i.e., Shap-E [41]) to generate coarse 3D instances, converts them into point clouds, enhances the point clouds via noisy point growth and color perturbation for 3D Gaussians initialization, and further optimizes the 3D Gaussians using SDS. This pipeline achieves real-time rendering and generates 3D instances on a single GPU within 15 minutes. Several works employ hybrid 3D representations, such as DM Tet, for object modeling. Specifically, Fantasia3D [14] decouples object geometry and texture. For geometry, it encodes extracted surface normals into the input of an image diffusion model; for texture, it introduces spatially varying BRDFs to learn surface materials for physics-based rendering. To address the low-resolution output issue of DreamFusion, Magic3D [15] adopts a two-stage optimization framework: first obtaining a coarse model via low-resolution diffusion priors and a hash-grid-encoded neural field, then refining it into a high-resolution textured 3D mesh using latent diffusion models (such as Stable Diffusion [129]). DreamCraft3D [17] decomposes object generation into two stages: geometric sculpting and texture boosting.

Improved Variant of SDS. Although SDS-based 3D generation methods demonstrate significant advantages in geometric representation optimization, their inherent defect of pseudo-ground-truth (pseudo-GT) distribution inconsistency leads to degraded quality and over-smoothing in model outputs. A series of representative works have proposed variants to tackle these shortcomings, as summarized in Table 3. Yu et al. [35] revealed that the effectiveness of SDS stems from its two gradient components: the generative prior $\hat{\epsilon}_\phi(x_t; y, t) - \epsilon$ and the classifier score $\hat{\epsilon}_\phi(x_t; y, t) - \hat{\epsilon}_\phi(x_t; \emptyset, t)$. Experiments demonstrate that SDS heavily depends on classifier-free guidance, causing the classifier score to dominate the optimization direction while the generative prior contributes minimally. Consequently, Classifier Score Distillation (CSD) discards the generative prior and solely uses the classifier score for optimization. LucidDreamer [143] introduces Interval Score Matching (ISM) to improve SDS. This method first employs DDIM inversion to generate reversible diffusion trajectories, reducing the averaging effect caused by pseudo-GT inconsistency. Additionally, ISM

matches between two interval steps along the diffusion trajectory, avoiding high reconstruction errors from single-step optimization. As an extension, GaussianDreamerPro [144] addresses the blurry edges in GaussianDreamer [69] by binding Gaussians to the surface of base 3D assets. By incorporating geometric constraints and optimizing Gaussian ellipsoids via ISM, it generates enhanced 3D objects. SDS also faces challenges with over-saturation and low diversity. To overcome these limitations, ProlificDreamer [37] proposes Variational Score Distillation (VSD), which models 3D parameters θ as distributions and optimizes their distribution via particle variational inference. Combined with low rank adaptation (LoRA) [145, 146] driven score estimation, VSD achieves more precise optimization directions. The latest work, ScaleDreamer [38], points out that VSD's reliance on LoRA fine-tuning compromises the generalization ability of pre-trained models to diverse text prompts, leading to training instability and mode collapse. Asynchronous Score Distillation (ASD) aims to resolve these issues by exploiting the observation that diffusion models exhibit lower noise prediction errors at earlier timesteps. By shifting the current timestep t forward to $t + \Delta t$, ASD reduces noise prediction errors without altering the pre-trained model weights, thus maintaining the model's capabilities while generating high-quality and diverse 3D content.

Multi-view Consistency Generation. The text-to-3D generation task faces significant modal mismatch challenges, rooted in the inherent contradiction between the sparsity of textual semantic guidance and the high-dimensional complexity of 3D geometric space. In contrast, the image-to-3D generation paradigms effectively enhances controllability by introducing strong visual priors. However, due to the lack of multi-view semantic associations and insufficient 3D geometric awareness, 2D lifting approaches often encounter the multi-face Janus problem. To address this, numerous studies have attempted to fine-tune pre-trained diffusion models to generate multi-view consistent images from single images. MVDream [93] constructs a diffusion model capable of generating multi-view images conditioned on text prompts. Zero-1-2-3 [94] equips Stable Diffusion models with camera viewpoint control, enabling novel view synthesis from a single input image and specified camera transformations, which can be applied to 3D reconstruction tasks. Its successor, Zero123++ [95], refines the Stable Diffusion 2 v -model through multi-view layout generation, noise schedule adjustment, scaled reference attention, and global conditioning mechanisms to produce more compliant multi-view images. Magic123 [16] employs a coarse-to-fine pipeline, representing objects implicitly via NeRF in the coarse stage and switching to a DM Tet-based hybrid representation combined with 2D and 3D diffusion priors in the fine stage to generate 3D content from unposed single images. One-2-3-45 [62] and its derivative One-2-3-45++ [63] adopt Zero-1-2-3 as a multi-view diffusion model to generate 3D textured meshes from single images. GeoDream [147] integrates the aforementioned works. Specifically, it first extracts 3D geometric priors via One-2-3-45 [62], followed by optimization with multi-view diffusion models [93–95] combined with the VSD loss [37]. SyncDreamer [148] generates multiple images simultaneously during reverse diffusion by constructing shared noise predictors, synchronizing noise predictions via 3D-aware attention mechanism to ensure multi-view consistency. Wonder3D [76] trains a cross-domain diffusion model to generate multi-view consistent normal maps and color maps, which are fused through SDF optimization to reconstruct 3D object geometry. Based on the Wonder3D framework, CADDreamer [149] achieves the generation of structured Computer-Aided Design (CAD) models from single-view images, effectively addressing the issue of loose mesh structures generated by previous methods. To improve lighting realism, UniDream [96] builds an albedo-normal aligned multi-view diffusion model, combining a Transformer-based reconstruction model with SDS optimization to endow objects with Physically-Based Rendering (PBR) materials using Stable Diffusion. DMV3D [77] generates tri-plane representations end-to-end from text or single-image inputs. MVDiffusion++ [97] focuses on high-resolution dense view synthesis through a pose-free multi-view diffusion model and view dropout strategy. Despite these advances, existing methods

Table 4. Evaluation Metrics of single-view 3D object generation methods on GSO [75] dataset.

Methods	FID ↓	CLIP ↑	PSNR ↑	LPIPS ↓	CD ↓
Point-E [10]	123.70	0.741	15.60	0.308	0.099
Shap-E [41]	97.05	0.805	14.36	0.289	0.085
Zero-1-to-3 [94]	32.44	0.896	17.36	0.182	–
One-2-3-45 [62]	139.24	0.713	12.42	0.448	0.123
Magic123 [16]	34.06	0.901	18.68	0.159	0.113
DMV3D [77]	30.01	0.928	22.57	0.126	0.040

like SyncDreamer [148] and Wonder3D [76] still produce coarse geometry and low-resolution textures due to residual local inconsistencies and architectural limitations. In contrast, Unique3D [78] generates multi-view images and normal maps via a multi-view diffusion model, enhances resolution through multi-level upsampling, and reconstructs 3D meshes from high-resolution data using the instant and consistent mesh reconstruction algorithm. Fancy123 [150] eliminates multi-view ghosting artifacts via 2D deformation, resolving local inconsistencies. Recently, a new category of methods eschewing model fine-tuning has emerged, addressing the multi-face Janus problem in 2D-lifting generation by integrating coarse 3D priors. Representative examples include Sherpa3D [18], DreamControl [39] and Sculpt3D [40]. Current generative methods typically produce assets as monolithic representations without structural partitioning. PartGen [151] addresses this gap by segmenting object parts while ensuring their integrity and compatibility. Based on the GSO [75] dataset, we conducted a quantitative evaluation of selected single-view 3D object generation methods, with the results summarized in Table 4. The rendering quality was evaluated using FID, CLIP similarity score, PSNR, and LPIPS between rendered and GT images. Furthermore, CD metric was employed to measure geometric similarity.

Texture Painting. In addition to the research paradigm of joint geometry-texture generation for objects, several studies have focused on texture enhancement for given 3D geometric structures, known as "texture painting". Representative works include: TEXTure [152] builds upon a pre-trained depth-to-image diffusion model, integrating an inpainting diffusion model for texture generation, transfer, and editing. Mitchel et al. [79] contributes two innovations: 1) Field Latents, which encode texture orientations and intensities as tangent vector fields at mesh vertices; 2) a Field Latent Diffusion Model that learns denoising processes in the tangent vector field space using field convolution networks to process local features for new texture generation. Several methods utilize exploit multi-view information for texture synthesis. Specifically, Text2Tex [88] combines a depth-aware diffusion model with multi-view dynamic mask generation to progressively optimize texture consistency and local details. TexFusion [153] employs a Sequential Interleaved Multi-view Sampler (SIMS) to aggregate latent textures across multiple views, followed by denoising and decoding into RGB textures. TexGen [98] employs multi-view sampling with attention-guided cross-view generation strategies to ensure detail consistency and color coherence, while a texture-aware noise adjustment strategy integrates texture and text information into noise prediction optimization, effectively addressing texture seams and over-smoothing issues. Paint3D [99] proposes a coarse-to-fine framework: the coarse stage employs depth-aware 2D diffusion models to generate multi-view conditional images through depth rendering and projection, while the refinement stage addresses texture gaps and enhances resolution via UV inpainting and super-resolution modules. MaPa [42] decomposes 3D meshes into segments and utilizes pre-trained segment-controlled diffusion models to generate segment-aligned RGB images. These images classify materials and initialize material map parameters, which are then optimized through differentiable rendering modules in iterative multi-view material generation. Recent research efforts have been dedicated to generating textures

Table 5. Quantitative comparison of diffusion-based texture painting methods on the ShapeNet [80] dataset.

Methods	Average		Bench		Car		Chair		Table		Time
	FID↓	KID↓	FID↓	KID↓	FID↓	KID↓	FID↓	KID↓	FID↓	KID↓	
TEXTure [152]	169.82	7.94	152.53	5.28	236.58	18.52	119.71	2.86	170.46	5.11	132.21s
Text2Tex [88]	156.62	6.68	154.95	5.79	188.60	15.06	125.34	3.11	157.57	2.77	1005.58s
Paint3D [99]	135.25	4.67	104.16	1.68	204.22	13.06	104.64	2.24	127.98	1.71	231.56s
TexGaussian [43]	100.97	1.88	86.37	0.75	117.53	5.20	94.89	0.57	105.09	0.95	11.12s

with enhanced photorealism in physical properties and lighting conditions. Paint-it [100] integrates a neural reparameterized Deep Convolutional PBR framework with diffusion models to synthesize comprehensive texture maps including albedo, roughness, metallic, and normal components, enabling high-resolution rendering compatible with physical material rendering pipelines. Material Anything [101] introduces confidence masks to dynamically control lighting effects, ensuring physical plausibility of materials under varying illumination conditions. TexGaussian [43] incorporates lighting attributes into traditional 3DGS parameters to enable physically based rendering. To help readers better understand the diffusion-based texture painting methods, as shown in Table 5, we selected some representative works from the aforementioned studies and conducted a quantitative comparison using 50 samples from each of the four categories in the ShapeNet [80] test set. The evaluation metrics included FID and KID to assess the quality and diversity of the generated textures, along with inference time measurements.

5 3D SCENE GENERATION

The key of 3D scene generation lies in the collaborative construction of objects and spatial environments. From the perspective of generation granularity, existing methods can be categorized into two primary technical routes: The first approach employs layout guidance to assemble generated individual objects into coherent scenes, while the second adopts a holistic scene generation paradigm that directly extracts scene-level object-background joint representations through multi-view 2D image analysis. Distinct from these two generation model-dependent paradigms, rule-driven modeling achieves controllable generation of complex scene content through predefined finite rule sets. This section will systematically elaborate on these three categories of 3D scene generation paradigms, as illustrated in Figure 4.

5.1 Layout-guided compositional synthesis

Layout-guided compositional synthesis can be defined as a technical paradigm for constructing complete scenes through systematic multi-object combination. Such methods typically utilize either predefined scene layouts or those learned from model-extracted scene features to model spatial topological relationships between objects.

As an early exploration in indoor scene synthesis, Wang et al. [154] adopted autoregressive decision-making to progressively construct complex layouts. Specifically, this method converts 3D scenes into orthographic top-down views and extracts spatial features via CNNs. At each generation step, it comprehensively considers the current scene state to gradually accomplish key operations including object category selection, instance retrieval, orientation adjustment, and collision detection. Through iterative updates of spatial geometric priors, this approach effectively ensures the rationality of scene layouts. In recent years, research utilizing scene layouts as spatial geometric priors has shown a diversified development trend. RoomDesigner [105] adopts lightweight anchor-latent variables to represent furniture attributes, leveraging Transformer architectures to autoregressively predict furniture features that are decoded into specific shapes and rationally arranged. PhyScene [109] seamlessly integrates collision avoidance, room layout, and accessibility

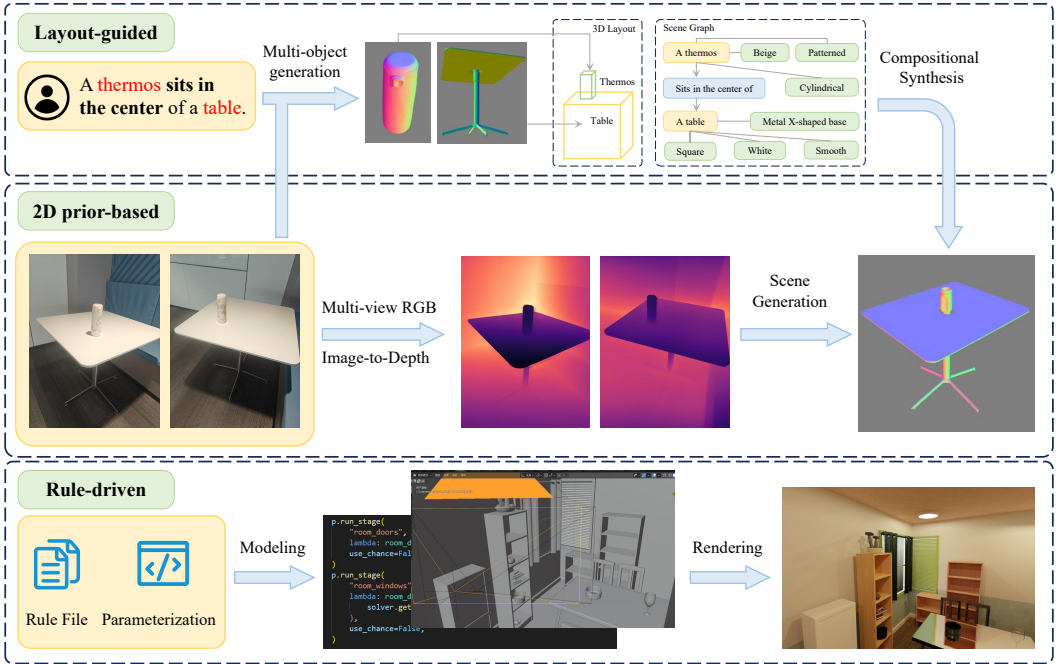


Fig. 4. Three major paradigms of 3D scene generation methods.

constraints into the diffusion process, exploring physical plausibility and interactivity in 3D indoor scene synthesis while providing high-quality training data for embodied AI. DiffuScene [106] innovatively parameterizes scene objects as feature vectors (including position, size, orientation, semantic category, and geometry), employing forward diffusion and reverse denoising processes to learn global scene layouts. This framework supports scene completion, object rearrangement, and text-conditioned generation. Similarly, focusing on text-driven indoor scene synthesis, InstructScene [44] achieves higher-fidelity controllable scene generation through the synergy of semantic map priors and layout decoders.

The generation of large-scale outdoor scenes faces challenges including high complexity of 3D spatial structures, vast scene scale, and scarcity of real-world datasets. To address these challenges, recent research has focused on leveraging layout and geometric knowledge provided by bird's-eye view (BEV) maps for outdoor scene generation. SceneDreamer [155] pioneers BEV representation for scene structures. Based on a GAN framework, it generates photorealistic unbounded 3D natural landscapes from random simplex noise and style codes. Both CityDreamer [156] and GaussianCity [157] focus on urban landscape generation rather than wilderness scenes, adopting BEV representations with divergent technical implementations. Specifically, the former employs a decoupled generation strategy, decomposing cities into three independent modules: unbounded layouts, background environments, and building instances, ultimately fused via a compositor. The latter further converts BEV into compact point cloud representations, significantly reducing memory consumption and achieving nearly 60× performance improvement over CityDreamer. Addressing infinite scene expansion demands, BerfScene [110] introduces BEV maps as layout priors, leveraging an equivariant U-Net architecture with low-pass filters and dynamic padding strategies to achieve seamless local scene stitching, effectively overcoming spatial boundary constraints.

Recent research in complex scene generation demonstrates significant trends toward cross-scene generalizability and multi-object compositional optimization. These methods transcend the limitations of indoor or outdoor scenes, focusing on collaborative object arrangement and globally

consistent synthesis to establish unique technical paradigms. Po et al. [158] introduces a joint control mechanism combining 3D bounding boxes with text prompts, implementing regional denoising strategies based on Voxel NeRF representations to enhance spatial controllability. DisCoScene [111] innovatively models scenes as semantic-agnostic 3D bounding box collections containing affine transformation parameters, thereby decoupling scene objects from backgrounds. Leveraging a GAN framework, it generates individual object radiance fields guided by layout priors, ensures photorealism through global-local discriminators, and supports object-level editing. For handling complex multi-object compositions, both Epstein et al. [159] and ComboVerse [160] adopt object-disentangled optimization paradigms. By independently optimizing object representations before learning spatial affine transformation parameters, they achieve semantically constrained scene compositions. Similarly, DreamDissector [161] introduces neural category fields to decompose NeRF density fields into category-specific sub-NeRFs. Enhanced by deep concept mining for disentanglement accuracy, it converts sub-NeRFs into DMTet-structured meshes, establishing a novel representation framework for component-wise complex scene generation. In contrast to the aforementioned approaches, Zhang et al. [162] discards complex generative models and instead learns spatial relationship priors combined with template optimization. This paradigm ensures layout rationality while achieving real-time generation efficiency at the second level.

Notably, LLMs have emerged as a research hotspot in scene synthesis due to their powerful text comprehension and contextual reasoning capabilities. SceneTeller [22] utilizes LLMs to parse positional and directional information from natural language, constructs layouts, and retrieves matching furniture models from 3D databases. The generated scenes are then represented via 3DGS and stylized using diffusion models. Similar to SceneTeller, studies including [23–26] extensively exploit LLMs’ semantic comprehension capabilities to extract critical scene elements from textual prompts. Specifically, SceneWiz3D [23] employs LLMs to disentangle objects and environments, representing them via DMTet and NeRF respectively. It automatically configures scene layouts through particle swarm optimization and optimizes scenes via SDS with perspective RGB and panoramic RGBD views. GALA3D [24] generates scene layouts based on LLM-parsed object topology relationships. Building upon instance Gaussian distributions from MVDream [93], it introduces adaptive geometry control modules to refine shape features and optimizes entire scenes via scene-level diffusion priors. DreamScene [25] decomposes scene prompts into object and environment descriptions, initializes object representations with sparse point clouds from Point-E [10], and refines 3DGS through multi-timestep sampling and CSD loss [35]. Gaussian filtering and texture refinement are applied alongside distinct three-stage camera sampling strategies for indoor/outdoor scenarios to produce high-quality, globally consistent, and editable 3D scenes.

Furthermore, scene graphs can also serve as intermediate state representations for layouts. A representative work, CommonScenes [112], employs a dual-branch generation framework where a VAE predicts scene layouts while a latent diffusion model jointly generates diverse 3D object shapes, ensuring global consistency and local relational rationality. Subsequent studies EcoScene [163] and MMGDreamer [45] propose dual-branch diffusion models for shape and layout generation. The former further supports dynamic editing of nodes and edges in scene graphs, while the latter enhances scene graph expressiveness through multimodal node and relation prediction, enabling finer control over scene layouts and object shapes. SceneCraft [164] generates executable Blender Python scripts by constructing scene graphs, converting object relationships into numerical constraints for asset layout, and iteratively synthesizing scenes through model retrieval. To address attribute confusion and guidance collapse in complex scenes for existing text-to-3D methods, GraphDreamer [26] converts text into scene graphs, combining node-level disentangled modeling with edge relationship constraints. This approach optimizes SDF representations through SDS loss and geometric constraints to generate composable 3D scenes. To achieve physically plausible

Table 6. Comparison of image and render quality across different scene generation approaches based on 2D priors.

Method	Image Quality				Render Quality		
	CLIP-Score \uparrow	Sharp \uparrow	Colorful \uparrow	Resolution \uparrow	PSNR \uparrow	SSIM \uparrow	LPIPS \downarrow
Text2Room [117]	-	-	-	-	19.29	0.728	0.206
LucidDreamer [36]	0.2110	0.9437	0.3230	0.4757	29.56	0.922	0.039
SceneDreamer360 [70]	0.2534	0.9877	0.3602	0.7082	35.74	0.963	0.035

complex scene synthesis, PhiP-G [165] designs multiple specialized agents: a keyword extraction agent constructs scene graphs from textual descriptions; a generation agent rapidly produces 3D assets; a classification agent precisely matches physical relationships between objects to ensure proper contact and fitting; and a supervision agent optimizes the overall scene through multi-view assessment of the layout.

5.2 2D prior-based scene generation

The 2D prior-based scene generation paradigm has emerged as a dominant research direction. These methods typically sample camera poses to generate multi-view RGB images for capturing texture and semantic information, integrate image-to-depth models to acquire depth maps for spatial layout estimation, and ultimately fuse multi-view RGB-D data to synthesize complete 3D point clouds or mesh models. As an early work in this domain, Shi et al. [166] proposed a dual-path generator architecture based on GANs to simultaneously synthesize RGB images and depth maps for indoor scenes. By designing a switchable discriminator that jointly supervises RGBD image realism and depth prediction tasks, this approach significantly enhanced 3D consistency and image quality. GAUDI [167] leverages input RGB-D images and camera pose information to learn the latent distribution of 3D scenes via a DDPM [140], enabling both unconditional and conditional 3D scene generation, yet it is constrained by low efficiency in both inference and rendering processes. NeuralField-LDM [168] employs a hierarchical latent diffusion framework to encode RGB images and camera poses into multi-level latent vectors, learning 3D scene distributions through staged diffusion processes, but its intermediate dense voxel grid representations incur sampling inefficiency and high training costs. RGBD2 [29] employs intermediate meshes for rendering and fusion, utilizing diffusion models for incremental view inpainting to fill missing details, ultimately generating multi-view consistent 3D indoor scenes from sparse RGBD inputs. Similarly, Text2Room [117] iteratively synthesizes indoor scenes through monocular depth estimation and view inpainting. SceneCraft [46] trains a 2D diffusion model with multi-view images containing semantic categories and depth information, learning a NeRF as the final scene representation. Text2NeRF [169] establishes a joint framework combining text-to-image diffusion models with NeRF, synthesizing multi-view consistent 3D scenes through progressive inpainting strategies. LucidDreamer [36] transforms multimodal inputs into multi-view aligned image collections, lifts 2D pixels to 3D space via depth estimation to construct initial point cloud representations, and iteratively optimizes 3DGS scene representations through reprojection refinement. The latest work WonderWorld [48] addresses the efficiency bottlenecks caused by existing methods' reliance on multi-view and depth map progressive generation as well as global scene optimization. By adopting a layered Gaussian surface representation to initialize scene geometry and facilitate rapid optimization. Additionally, this method introduces scene visible depth as a constraint to mitigate geometric seam artifacts, there by achieving second-level generation of interactive 3D scenes.

Compared to the stitching of multiple single-view images, panoramas often provide more comprehensive and geometrically consistent knowledge. The following works all adopt panoramic images

as 2D visual priors. RoomDreamer [170] generates 360° panoramic images based on text prompts and geometric guidance, and supplements uncovered regions via diffusion models. Building upon the generated 2D images, the geometry and texture of a 3D mesh are jointly optimized, leveraging monocular depth estimation as pseudo-supervision to smooth geometry and inpaint holes. Unlike iterative view inpainting with predefined camera poses in RGBD2 [29], GenRC [47] directly synthesizes cross-view consistent panoramic RGBD images using a pre-trained diffusion model and a custom E-Diffusion technique, thereby completing scene geometry and texture. To address the complexity of manual 3D environment creation and the unreasonable layouts in existing automated 3D room mesh generation methods, ControlRoom3D [119] represents objects as 3D semantic proxy rooms, employs latent diffusion models to generate panoramas with depth estimation for layout alignment, and iteratively refines mesh shapes and textures. Diverging from the above methods that extract meshes from images, DreamScene360 [171] and SceneDreamer360 [70] adopt 3DGS for scene representation. The former lifts 2D panoramas to 3DGS for globally consistent 3D scene generation. The latter first generates text-driven panoramas, enhances their resolution via multi-view algorithms, and utilizes monocular depth estimation models to provide depth maps for initial point cloud fusion and alignment. Finally, 3DGS is trained on the initialized point cloud to achieve high-fidelity 3D scenes. Table 6 presents the quantitative comparison of some scene generation methods based on 2D priors. The CLIP-Score metric is employed to measure text-image alignment, while CLIP-IQA (e.g., Sharp, Colorful, Resolution) [172] provides human-perception-aligned image quality assessment.

Analogous to object texture painting, SceneTex [113] specializes in generating textures for given indoor scene geometries. This method encodes multi-scale texture features through multi-resolution atlases, resolves style inconsistencies caused by viewpoint variations and self-occlusions via multi-head cross-attention mechanisms, and employs depth-to-image models to render RGB images. Leveraging VSD [37] for gradient computation and texture field updates, it achieves text-to-high-fidelity indoor scene texture synthesis. Notably, while existing diffusion models excel in optical image generation, they struggle to synthesize LiDAR scenes containing complex structures like roads, vehicles, buildings, and terrains. This type of data holds significant value in areas such as autonomous driving and archaeology. Addressing this gap, Ran et al. [173] proposes the first multi-modal conditional LiDAR diffusion model supporting joint inputs of semantic maps, camera views, and text prompts, pioneering technological advancements in this domain.

5.3 Rule-driven modeling

Rule-driven modeling is a technique for automatically creating 3D models and textures based on predefined rules, parametric systems, and mathematical functions. This approach enables controllable generation of complex and diverse content (e.g., terrains, buildings, vegetation) through finite rule sets, with its core advantage lying in rapid and efficient content production without reliance on large-scale data training. However, designing low complexity yet highly robust generation rules remains a primary challenge in this field. The academic community has conducted systematic research and achieved significant progress in this domain.

As one of the earliest attempts at rule-based modeling, L-system [1] serves as a formal language system for simulating biological growth processes. It generates intricate structures through recursive string replacement rules and has been widely applied in plant modeling and fractal geometry, establishing itself as a foundational tool for procedural modeling. Parish et al [2] expanded on L-system to develop the CityEngine system, which pioneered rule-driven generation of roads, parcels, and buildings for urban scenes using minimal statistical and geographical input data. Building upon this work, Müller et al. [3] introduced CGA shape, enabling efficient generation of

high-detail 3D cities from simple volumetric models through extended shape grammars and context-sensitive rules. Their implementation integrated CGA shapes into the CityEngine framework using C++. Lipp et al. [174] and Vanegas et al. [175] focused on urban layout generation. The former combined hierarchical systems with graph-cut algorithms for iterative layout merging, integrating procedural generation with interactive editing to ensure layout validity. The latter proposed a compositional approach by independently generating and assembling urban parcels. Talton et al. [176] innovatively incorporated Markov chain Monte Carlo (MCMC) techniques into grammar-driven modeling, achieving automatic rule optimization through probabilistic inference to reduce manual design complexity.

Recent work includes Merrell and Paul [177]’s graph grammar-based example-driven procedural modeling method. By decomposing example shapes into primitives and automatically deriving grammar rules, this approach achieves locally similar yet globally diverse shape generation, supporting 2D/3D extensions for complex structures such as architecture and natural landscapes. Raistrick et al. [30] developed a mathematical rule-driven generation framework that parameterizes geometric shapes, textures, and materials to enable infinite combinations of natural assets (e.g., terrains, flora, fauna), seamlessly integrated with Blender [178]. Their subsequent work *Infinigen Indoors* [179] specializes in indoor scene generation, supporting dynamic mesh detail adjustment based on depth of field and user-defined complex layout constraints.

With the rise of language and vision models, modern procedural modeling increasingly follows a pipeline of 3D feature extraction from existing tools to generate rules/grammars, which then drive asset creation. Specifically, 3D-GPT [27] parses textual inputs via LLMs to select procedural functions from the *Infinigen* library and generate executable Blender Python scripts, enabling dynamic editing and photorealistic rendering of natural scenes. *SceneX* [180] integrates 172 procedural modules and 11,284 static 3D assets with standardized APIs, combining LLM-driven planners for scene decomposition and asset placement to create controlled natural scenes and unbounded cities. *CityX* [181] employs procedural modules and multi-agent collaboration frameworks to generate photorealistic 3D urban environments from multimodal inputs (e.g., text descriptions, OSM files, semantic maps). *Proc-GS* [49] integrates 3DGS into the procedural pipeline, using 3DGS for editable asset extraction during acquisition and LLM optimization of procedural codes for flexible asset composition during assembly. Feng et al. [28] utilize LLMs to parse scene features from text, derive 2D layouts, heightmaps, and textures through 3D layout generation modules, and dynamically adjust predefined CGA templates via LLMs to map 2D layouts and model features into fully editable 3D urban environments in *CityEngine* [182].

6 CHALLENGE AND FUTURE WORK

Benefiting from the emergence of novel 3D representations and advances in generative models, 3D generation methods have achieved significant technical breakthroughs. However, substantial obstacles persist in effectively applying the generated content to downstream tasks. This section discusses the remaining challenges in this realm and identifies potential future research directions.

6.1 3D Data

In recent years, the rapid advancement of language models and vision models has significantly improved the efficiency of constructing text and 2D image datasets, where data sources encompass both naturally collected samples and synthetically generated content through generative models. However, the creation and acquisition of 3D assets still face critical challenges: professional-grade 3D modeling relies on manual design by artists using specialized software or high-precision scanning equipment, leading to prohibitively high data acquisition costs. These constraints have resulted in current publicly available 3D datasets exhibiting notable limitations, including restricted

Table 7. Quantitative comparisons on T³Bench [183]. The score is the mean of two evaluation metrics (quality and alignment).

Methods	Running Time ↓	Single Obj. ↑	Single w/Surr. ↑	Multi Obj. ↑	Average ↑
DreamFusion [21]	30minutes	24.4	24.6	16.1	21.7
Fantasia3D [14]	45minutes	26.4	27.0	18.5	24.0
Magic3D [15]	40minutes	37.0	35.4	25.7	32.7
ProlificDreamer [37]	240minutes	49.4	44.8	35.8	43.3
MVDream [93]	30minutes	47.8	42.4	33.8	41.3
DreamGaussian [68]	7minutes	19.8	14.1	10.9	14.9
GeoDream [147]	400minutes	41.1	34.9	25.4	33.8
GaussianDreamer [69]	-	54.0	48.6	34.5	45.7

object categories and insufficient geometric details, which fail to meet the demands of complex 3D generation tasks.

Although many studies [21, 35–38, 48, 143, 169] have promoted the development of 3D generation methods based on 2D prior knowledge, the establishment of large-scale, high-quality 3D datasets remains irreplaceable in value. On one hand, such datasets can provide reliable benchmarks for training and validation of data-driven and generative model-based 3D generation algorithms. On the other hand, standardized datasets will facilitate quantitative evaluation and comparative studies within the 3D generation research community.

6.2 Evaluation metrics

Establishing a quantitative evaluation system for assessing the quality of 3D content generation remains one of the major challenges in the field of 3D generation. Current evaluation metrics are broadly classified into two categories: objective and subjective measurements.

Objective evaluation primarily focuses on quantifiable metrics. Traditional image quality assessment methods such as PSNR, SSIM, and LPIPS, along with generative adversarial network metrics including FID and KID, are employed to evaluate the rendered outputs of generated content. However, these 2D projection-based evaluation methods struggle to comprehensively capture the geometric consistency and diversity characteristics of 3D content. For geometric similarity measurement, metrics such as Chamfer Distance (CD) and Intersection over Union (IoU) assess geometric accuracy by quantifying point set or voxel differences between generated shapes and reference ground truth. Nevertheless, these metrics not only rely on ground truth data but also may inadequately reflect topological structures or fine-grained surface quality. Recent advancements have introduced multimodal evaluation methods based on CLIP models. CLIP Score [184] is employed to quantify the semantic alignment between text and 3D content (or its rendered images). As a text-to-3D generation benchmark, T³Bench [183] comprises three categories of text prompts: single objects, single objects with surrounding environments, and multiple objects. By introducing an automated evaluation framework that addresses two critical dimensions: 3D subjective quality assessment and text alignment evaluation, this benchmark effectively enhances the comparability of generation methods. Building upon this framework, we present qualitative comparisons of various diffusion-based generation approaches, as shown in Table 7.

Subjective evaluation predominantly relies on user studies, which integrate human geometric cognition and visual perception capabilities to holistically assess the quality and diversity of generated content. However, this approach is not only time-consuming and labor-intensive but also subject to evaluators' subjective preferences, thereby compromising the objectivity and reproducibility of assessment outcomes.

Currently, a unified evaluation standard system has yet to be established. The development of a multi-dimensional evaluation framework that simultaneously addresses geometric precision, physical plausibility, and semantic consistency holds urgent theoretical significance and practical value for advancing 3D content generation technologies.

6.3 Potential Research Direction

3D generation, as a key technology in computer graphics and vision, holds significant application value in cutting-edge scenarios. Although contemporary 3D content generation methods have achieved remarkable progress in output quality, diversity, and efficiency, they still exhibit critical limitations regarding object controllability, physical plausibility, and the capacity to handle large-scale and complex scenes. Consequently, the practical implementation of these generative outcomes in real-world applications poses formidable challenges.

Regarding controllability, current automated generation tools, particularly deep generative models, whether employing unconditional generation or conditional generation based on text/image inputs, demonstrate that existing architectures still struggle to fully reproduce the geometric details and appearance characteristics anticipated by users. In contrast, rule-driven procedural modeling offers excellent controllability, yet the complexity of designing rule systems and the difficulty of algorithmic implementation significantly raise the technical entry barrier. Further utilization of mature tools such as language and vision models to extract scene features for rule generation, thereby enabling inverse procedural modeling [4, 5], represents a potential future research direction. From a physical plausibility perspective, recent work PhysGen3D [185] infer the physical parameters of objects from single images, ensuring their motion adheres to real-world physical laws. This framework supports user-defined properties to enable precise control over scene interaction effects. RainyGS [186] integrates the accuracy of physical rain simulation with the efficient rendering capabilities of 3DGS. Through splash simulation and particle collision detection, it achieves efficient synthesis of physically credible rainy scenes in open environments. These explorations demonstrate the potential of combining physical constraints with generative models. However, research on object/scene interaction and the modeling of physical properties for generated objects still requires deeper investigation.

Furthermore, the generation and extension of unbounded scenes warrant in-depth discussion. The core objective lies in developing algorithms or models capable of generating infinitely extensible 3D scenes or seamlessly expanding and integrating existing finite scenes. Key challenges in this field primarily involve two aspects: First, explicit 3D representations struggle to address the storage and transmission demands of infinite scenes, necessitating research into implicit representation frameworks and efficient data compression methodologies. Second, it is imperative to ensure structural and textural consistency between extended regions and original scenes to prevent visual discontinuities. Addressing these challenges, some works [110, 155–157] have explored unbounded natural landscapes and urban environments. Emerging studies indicate that divide-and-conquer strategies combined with multi-scale modeling can effectively decompose scene complexity. Specifically, LT3SD [114] decomposes 3D scenes into hierarchical latent tree structures, where each layer contains geometric volumes and latent feature volumes to capture low-frequency information while encoding high-frequency details. During training, it randomly crops scene patches to learn shared local structural features. At inference, it employs a fine-to-coarse block generation strategy to enable unbounded indoor scene expansion. Liu et al. [187] investigates diffusion models for large-scale outdoor 3D scene synthesis. Inspired by pyramid-based multi-scale modeling, this approach decomposes scenes into multiple scales, each governed by an independent diffusion model. The system progressively refines local features based on coarse-grained scene layouts, utilizing scene partitioning to overcome GPU memory constraints and theoretically supporting

infinite-scale scene generation. BlockFusion [107] generates high-quality 3D scene geometry through tri-plane compression and latent space diffusion, achieving infinite scene expansion via extrapolation mechanisms.

Finally, in terms of scene visualization effectiveness, while neural representations [9] based on volume rendering achieve high-fidelity visual quality, their compatibility challenges with rasterization-based graphics pipelines hinder direct integration into traditional workflows like game engines. Emerging techniques like 3DGS have improved real-time performance, yet they still exhibit limitations in material expressiveness under complex illumination conditions. Furthermore, real-time rendering of unbounded scenes necessitates the integration of level-of-detail systems, view frustum culling, and asynchronous loading mechanisms to balance detail precision with computational resources. Future research could focus on the efficient generation of complex scenes while also exploring real-time rendering techniques.

7 CONCLUSION

This paper presents a comprehensive review on 3D object and scene generation. We commence by investigating fundamental theoretical frameworks of 3D representations, analyzing their critical impacts on the quality of generative algorithms and computational efficiency. Subsequently, we systematically classify and summarize of 3D object generation methods. Expanding the scope to complex scene levels, we then elaborate on the technical evolution of 3D scene generation approaches. The survey concludes with an in-depth discussion of unresolved challenges in this field and proposes potential research directions for future exploration. Through this systematic examination, we aim to establish a structured technical reference framework for 3D content generation, providing both theoretical foundations and technical insights to facilitate subsequent research advancements.

REFERENCES

- [1] Aristid Lindenmayer. 1968. Mathematical models for cellular interactions in development I. Filaments with one-sided inputs. *Journal of theoretical biology* 18, 3 (1968), 280–299.
- [2] Yoav IH Parish and Pascal Müller. 2001. Procedural modeling of cities. In *Proceedings of the 28th annual conference on Computer graphics and interactive techniques*. 301–308.
- [3] Pascal Müller, Peter Wonka, Simon Haegler, Andreas Ulmer, and Luc Van Gool. 2006. Procedural modeling of buildings. In *ACM SIGGRAPH 2006 Papers*. 614–623.
- [4] Jianwei Guo, Haiyong Jiang, Bedrich Benes, Oliver Deussen, Xiaopeng Zhang, Dani Lischinski, and Hui Huang. 2020. Inverse procedural modeling of branching structures by inferring l-systems. *ACM Transactions on Graphics (TOG)* 39, 5 (2020), 1–13.
- [5] Albert J Zhai, Xinlei Wang, Kaiyuan Li, Zhao Jiang, Junxiong Zhou, Sheng Wang, Zhenong Jin, Kaiyu Guan, and Shenlong Wang. 2024. CropCraft: Inverse Procedural Modeling for 3D Reconstruction of Crop Plants. *arXiv preprint arXiv:2411.09693* (2024).
- [6] Daya Guo, Dejian Yang, Haowei Zhang, Junxiao Song, Ruoyu Zhang, Runxin Xu, Qihao Zhu, Shirong Ma, Peiyi Wang, Xiao Bi, et al. 2025. Deepseek-r1: Incentivizing reasoning capability in llms via reinforcement learning. *arXiv preprint arXiv:2501.12948* (2025).
- [7] Chitwan Saharia, William Chan, Saurabh Saxena, Lala Li, Jay Whang, Emily L Denton, Kamyar Ghasemipour, Raphael Gontijo Lopes, Burcu Karagol Ayan, Tim Salimans, et al. 2022. Photorealistic text-to-image diffusion models with deep language understanding. *Advances in neural information processing systems* 35 (2022), 36479–36494.
- [8] Aaron Hurst, Adam Lerer, Adam P Goucher, Adam Perelman, Aditya Ramesh, Aidan Clark, AJ Ostrow, Akila Welihinda, Alan Hayes, Alec Radford, et al. 2024. Gpt-4o system card. *arXiv preprint arXiv:2410.21276* (2024).
- [9] Ben Mildenhall, Pratul P Srinivasan, Matthew Tancik, Jonathan T Barron, Ravi Ramamoorthi, and Ren Ng. 2021. Nerf: Representing scenes as neural radiance fields for view synthesis. *Commun. ACM* 65, 1 (2021), 99–106.
- [10] Alex Nichol, Heewoo Jun, Prafulla Dhariwal, Pamela Mishkin, and Mark Chen. 2022. Point-e: A system for generating 3d point clouds from complex prompts. *arXiv preprint arXiv:2212.08751* (2022).
- [11] Jeong Joon Park, Peter Florence, Julian Straub, Richard Newcombe, and Steven Lovegrove. 2019. DeepSDF: Learning continuous signed distance functions for shape representation. In *Proceedings of the IEEE/CVF conference on computer*

vision and pattern recognition. 165–174.

- [12] Andrew Luo, Tianqin Li, Wen-Hao Zhang, and Tai Sing Lee. 2021. Surfgen: Adversarial 3d shape synthesis with explicit surface discriminators. In *Proceedings of the IEEE/CVF international conference on computer vision.* 16238–16248.
- [13] Jun Gao, Tianchang Shen, Zian Wang, Wenzheng Chen, Kangxue Yin, Daiqing Li, Or Litany, Zan Gojic, and Sanja Fidler. 2022. Get3d: A generative model of high quality 3d textured shapes learned from images. *Advances In Neural Information Processing Systems* 35 (2022), 31841–31854.
- [14] Rui Chen, Yongwei Chen, Ningxin Jiao, and Kui Jia. 2023. Fantasia3d: Disentangling geometry and appearance for high-quality text-to-3d content creation. In *Proceedings of the IEEE/CVF international conference on computer vision.* 22246–22256.
- [15] Chen-Hsuan Lin, Jun Gao, Luming Tang, Towaki Takikawa, Xiaohui Zeng, Xun Huang, Karsten Kreis, Sanja Fidler, Ming-Yu Liu, and Tsung-Yi Lin. 2023. Magic3d: High-resolution text-to-3d content creation. In *Proceedings of the IEEE/CVF conference on computer vision and pattern recognition.* 300–309.
- [16] Guocheng Qian, Jinjie Mai, Abdullah Hamdi, Jian Ren, Aliaksandr Siarohin, Bing Li, Hsin-Ying Lee, Ivan Skorokhodov, Peter Wonka, Sergey Tulyakov, et al. 2023. Magic123: One image to high-quality 3d object generation using both 2d and 3d diffusion priors. *arXiv preprint arXiv:2306.17843* (2023).
- [17] Jingxiang Sun, Bo Zhang, Ruizhi Shao, Lizhen Wang, Wen Liu, Zhenda Xie, and Yebin Liu. 2023. Dreamcraft3d: Hierarchical 3d generation with bootstrapped diffusion prior. *arXiv preprint arXiv:2310.16818* (2023).
- [18] Fangfu Liu, Diankun Wu, Yi Wei, Yongming Rao, and Yueqi Duan. 2024. Sherpa3d: Boosting high-fidelity text-to-3d generation via coarse 3d prior. In *Proceedings of the IEEE/CVF Conference on Computer Vision and Pattern Recognition.* 20763–20774.
- [19] William E Lorensen and Harvey E Cline. 1998. Marching cubes: A high resolution 3D surface construction algorithm. In *Seminal graphics: pioneering efforts that shaped the field.* 347–353.
- [20] Akio Doi and Akio Koide. 1991. An efficient method of triangulating equi-valued surfaces by using tetrahedral cells. *IEICE TRANSACTIONS on Information and Systems* 74, 1 (1991), 214–224.
- [21] Ben Poole, Ajay Jain, Jonathan T Barron, and Ben Mildenhall. 2022. Dreamfusion: Text-to-3d using 2d diffusion. *arXiv preprint arXiv:2209.14988* (2022).
- [22] Başak Melis Ocal, Maxim Tatarchenko, Sezer Karaoğlu, and Theo Gevers. 2024. SceneTeller: Language-to-3D Scene Generation. In *European Conference on Computer Vision.* Springer, 362–378.
- [23] Qihang Zhang, Chaoyang Wang, Aliaksandr Siarohin, Peiye Zhuang, Yinghao Xu, Ceyuan Yang, Dahua Lin, Bolei Zhou, Sergey Tulyakov, and Hsin-Ying Lee. 2024. Towards text-guided 3d scene composition. In *Proceedings of the IEEE/CVF Conference on Computer Vision and Pattern Recognition.* 6829–6838.
- [24] Xiaoyu Zhou, Xingjian Ran, Yajiao Xiong, Jinlin He, Zhiwei Lin, Yongtao Wang, Deqing Sun, and Ming-Hsuan Yang. 2024. Gala3d: Towards text-to-3d complex scene generation via layout-guided generative gaussian splatting. *arXiv preprint arXiv:2402.07207* (2024).
- [25] Haoran Li, Haolin Shi, Wenli Zhang, Wenjun Wu, Yong Liao, Lin Wang, Lik-hang Lee, and Peng Yuan Zhou. 2024. Dreamscene: 3d gaussian-based text-to-3d scene generation via formation pattern sampling. In *European Conference on Computer Vision.* Springer, 214–230.
- [26] Gege Gao, Weiyang Liu, Anpei Chen, Andreas Geiger, and Bernhard Schölkopf. 2024. Graphdreamer: Compositional 3d scene synthesis from scene graphs. In *Proceedings of the IEEE/CVF Conference on Computer Vision and Pattern Recognition.* 21295–21304.
- [27] Chunyi Sun, Junlin Han, Weijian Deng, Xinlong Wang, Zishan Qin, and Stephen Gould. 2023. 3d-gpt: Procedural 3d modeling with large language models. *arXiv preprint arXiv:2310.12945* (2023).
- [28] Yuchuan Feng, Jihang Jiang, Jie Ren, Wenrui Li, Ruotong Li, and Xiaopeng Fan. 2025. Text-Guided Editable 3D City Scene Generation. In *ICASSP 2025-2025 IEEE International Conference on Acoustics, Speech and Signal Processing (ICASSP).* IEEE, 1–5.
- [29] Jiabao Lei, Jiapeng Tang, and Kui Jia. 2023. Rgb2: Generative scene synthesis via incremental view inpainting using rgb2 diffusion models. In *Proceedings of the IEEE/CVF conference on computer vision and pattern recognition.* 8422–8434.
- [30] Alexander Raistrick, Lahav Lipson, Zeyu Ma, Lingjie Mei, Mingzhe Wang, Yiming Zuo, Karhan Kayan, Hongyu Wen, Beining Han, Yihan Wang, et al. 2023. Infinite photorealistic worlds using procedural generation. In *Proceedings of the IEEE/CVF conference on computer vision and pattern recognition.* 12630–12641.
- [31] Jinwoo Kim, Jaehoon Yoo, Juho Lee, and Seunghoon Hong. 2021. Setvae: Learning hierarchical composition for generative modeling of set-structured data. In *Proceedings of the IEEE/CVF Conference on Computer Vision and Pattern Recognition.* 15059–15068.
- [32] Paritosh Mittal, Yen-Chi Cheng, Maneesh Singh, and Shubham Tulsiani. 2022. Autosdf: Shape priors for 3d completion, reconstruction and generation. In *Proceedings of the IEEE/CVF conference on computer vision and pattern recognition.* 306–315.

- [33] Sijin Chen, Xin Chen, Anqi Pang, Xianfang Zeng, Wei Cheng, Yijun Fu, Fukun Yin, Billzb Wang, Jingyi Yu, Gang Yu, et al. 2024. Meshxl: Neural coordinate field for generative 3d foundation models. *Advances in Neural Information Processing Systems* 37 (2024), 97141–97166.
- [34] Florian Barthel, Arian Beckmann, Wieland Morgenstern, Anna Hilsman, and Peter Eisert. 2024. Gaussian splatting decoder for 3d-aware generative adversarial networks. In *Proceedings of the IEEE/CVF Conference on Computer Vision and Pattern Recognition*. 7963–7972.
- [35] Xin Yu, Yuan-Chen Guo, Yangguang Li, Ding Liang, Song-Hai Zhang, and Xiaojuan Qi. 2023. Text-to-3d with classifier score distillation. *arXiv preprint arXiv:2310.19415* (2023).
- [36] Jaeyoung Chung, Suyoung Lee, Hyeongjin Nam, Jaerin Lee, and Kyoung Mu Lee. 2023. Luciddreamer: Domain-free generation of 3d gaussian splatting scenes. *arXiv preprint arXiv:2311.13384* (2023).
- [37] Zhengyi Wang, Cheng Lu, Yikai Wang, Fan Bao, Chongxuan Li, Hang Su, and Jun Zhu. 2023. Prolificdreamer: High-fidelity and diverse text-to-3d generation with variational score distillation. *Advances in Neural Information Processing Systems* 36 (2023), 8406–8441.
- [38] Zhiyuan Ma, Yuxiang Wei, Yabin Zhang, Xiangyu Zhu, Zhen Lei, and Lei Zhang. 2024. Scaledreamer: Scalable text-to-3d synthesis with asynchronous score distillation. In *European Conference on Computer Vision*. Springer, 1–19.
- [39] Tianyu Huang, Yihan Zeng, Zhilu Zhang, Wan Xu, Hang Xu, Songcen Xu, Rynson WH Lau, and Wangmeng Zuo. 2024. Dreamcontrol: Control-based text-to-3d generation with 3d self-prior. In *Proceedings of the IEEE/CVF conference on computer vision and pattern recognition*. 5364–5373.
- [40] Cheng Chen, Xiaofeng Yang, Fan Yang, Chengzeng Feng, Zhoujie Fu, Chuan-Sheng Foo, Guosheng Lin, and Fayao Liu. 2024. Sculpt3d: Multi-view consistent text-to-3d generation with sparse 3d prior. In *Proceedings of the IEEE/CVF Conference on Computer Vision and Pattern Recognition*. 10228–10237.
- [41] Heewoo Jun and Alex Nichol. 2023. Shap-e: Generating conditional 3d implicit functions. *arXiv preprint arXiv:2305.02463* (2023).
- [42] Shangzhan Zhang, Sida Peng, Tao Xu, Yuanbo Yang, Tianrun Chen, Nan Xue, Yujun Shen, Hujun Bao, Ruizhen Hu, and Xiaowei Zhou. 2024. Mapa: Text-driven photorealistic material painting for 3d shapes. In *ACM SIGGRAPH 2024 Conference Papers*. 1–12.
- [43] Bojun Xiong, Jialun Liu, Jiakui Hu, Chenming Wu, Jinbo Wu, Xing Liu, Chen Zhao, Errui Ding, and Zhouhui Lian. 2024. TexGaussian: Generating High-quality PBR Material via Octree-based 3D Gaussian Splatting. *arXiv preprint arXiv:2411.19654* (2024).
- [44] Chenguo Lin and Yadong Mu. 2024. Instructscene: Instruction-driven 3d indoor scene synthesis with semantic graph prior. *arXiv preprint arXiv:2402.04717* (2024).
- [45] Zhifei Yang, Keyang Lu, Chao Zhang, Jiaying Qi, Hanqi Jiang, Ruifei Ma, Shenglin Yin, Yifan Xu, Mingzhe Xing, Zhen Xiao, et al. 2025. MMGDreamer: Mixed-Modality Graph for Geometry-Controllable 3D Indoor Scene Generation. *arXiv preprint arXiv:2502.05874* (2025).
- [46] Xiuyu Yang, Yunze Man, Junkun Chen, and Yu-Xiong Wang. 2024. SceneCraft: Layout-guided 3D scene generation. *Advances in Neural Information Processing Systems* 37 (2024), 82060–82084.
- [47] Ming-Feng Li, Yueh-Feng Ku, Hong-Xuan Yen, Chi Liu, Yu-Lun Liu, Albert YC Chen, Cheng-Hao Kuo, and Min Sun. 2024. GenRC: Generative 3D room completion from sparse image collections. In *European Conference on Computer Vision*. Springer, 146–163.
- [48] Hong-Xing Yu, Haoyi Duan, Charles Herrmann, William T Freeman, and Jiajun Wu. 2024. Wonderworld: Interactive 3d scene generation from a single image. *arXiv preprint arXiv:2406.09394* (2024).
- [49] Yixuan Li, Xingjian Ran, Linning Xu, Tao Lu, Mulin Yu, Zhenzhi Wang, Yuanbo Xiangli, Dahua Lin, and Bo Dai. 2024. Proc-GS: Procedural building generation for city assembly with 3D Gaussians. *arXiv preprint arXiv:2412.07660* (2024).
- [50] Zifan Shi, Sida Peng, Yinghao Xu, Andreas Geiger, Yiyi Liao, and Yujun Shen. 2022. Deep generative models on 3d representations: A survey. *arXiv preprint arXiv:2210.15663* (2022).
- [51] Chenghao Li, Chaoning Zhang, Joseph Cho, Atish Waghvase, Lik-Hang Lee, Francois Rameau, Yang Yang, Sung-Ho Bae, and Choong Seon Hong. 2023. Generative ai meets 3d: A survey on text-to-3d in aigc era. *arXiv preprint arXiv:2305.06131* (2023).
- [52] Chenhan Jiang. 2024. A Survey On Text-to-3D Contents Generation In The Wild. *arXiv preprint arXiv:2405.09431* (2024).
- [53] Lin Geng Foo, Hossein Rahmani, and Jun Liu. 2023. Ai-generated content (aigc) for various data modalities: A survey. *arXiv preprint arXiv:2308.14177* (2023).
- [54] Xiaoyu Li, Qi Zhang, Di Kang, Weihao Cheng, Yiming Gao, Jingbo Zhang, Zhihao Liang, Jing Liao, Yan-Pei Cao, and Ying Shan. 2024. Advances in 3d generation: A survey. *arXiv preprint arXiv:2401.17807* (2024).
- [55] Jian Liu, Xiaoshui Huang, Tianyu Huang, Lu Chen, Yuenan Hou, Shixiang Tang, Ziwei Liu, Wanli Ouyang, Wangmeng Zuo, Junjun Jiang, et al. 2024. A comprehensive survey on 3d content generation. *arXiv preprint arXiv:2402.01166* (2024).

- [56] Nanyang Wang, Yinda Zhang, Zhuwen Li, Yanwei Fu, Wei Liu, and Yu-Gang Jiang. 2018. Pixel2mesh: Generating 3d mesh models from single rgb images. In *Proceedings of the European conference on computer vision (ECCV)*. 52–67.
- [57] Georgia Gkioxari, Jitendra Malik, and Justin Johnson. 2019. Mesh r-cnn. In *Proceedings of the IEEE/CVF international conference on computer vision*. 9785–9795.
- [58] Yongbin Sun, Yue Wang, Ziwei Liu, Joshua Siegel, and Sanjay Sarma. 2020. Pointgrow: Autoregressively learned point cloud generation with self-attention. In *Proceedings of the IEEE/CVF Winter Conference on Applications of Computer Vision*. 61–70.
- [59] Aditya Sanghi, Hang Chu, Joseph G Lambourne, Ye Wang, Chin-Yi Cheng, Marco Fumero, and Kamal Rahimi Malekshan. 2022. Clip-forge: Towards zero-shot text-to-shape generation. In *Proceedings of the IEEE/CVF Conference on Computer Vision and Pattern Recognition*. 18603–18613.
- [60] Jiajun Wu, Chengkai Zhang, Tianfan Xue, Bill Freeman, and Josh Tenenbaum. 2016. Learning a probabilistic latent space of object shapes via 3d generative-adversarial modeling. *Advances in neural information processing systems* 29 (2016).
- [61] Yen-Chi Cheng, Hsin-Ying Lee, Sergey Tulyakov, Alexander G Schwing, and Liang-Yan Gui. 2023. Sdfusion: Multimodal 3d shape completion, reconstruction, and generation. In *Proceedings of the IEEE/CVF conference on computer vision and pattern recognition*. 4456–4465.
- [62] Minghua Liu, Chao Xu, Haiyan Jin, Linghao Chen, Mukund Varma T, Zexiang Xu, and Hao Su. 2023. One-2-3-45: Any single image to 3d mesh in 45 seconds without per-shape optimization. *Advances in Neural Information Processing Systems* 36 (2023), 22226–22246.
- [63] Minghua Liu, Ruoxi Shi, Linghao Chen, Zhuoyang Zhang, Chao Xu, Xinyue Wei, Hansheng Chen, Chong Zeng, Jiayuan Gu, and Hao Su. 2024. One-2-3-45++: Fast single image to 3d objects with consistent multi-view generation and 3d diffusion. In *Proceedings of the IEEE/CVF conference on computer vision and pattern recognition*. 10072–10083.
- [64] Lars Mescheder, Michael Oechsle, Michael Niemeyer, Sebastian Nowozin, and Andreas Geiger. 2019. Occupancy networks: Learning 3d reconstruction in function space. In *Proceedings of the IEEE/CVF conference on computer vision and pattern recognition*. 4460–4470.
- [65] Thomas Müller, Alex Evans, Christoph Schied, and Alexander Keller. 2022. Instant neural graphics primitives with a multiresolution hash encoding. *ACM transactions on graphics (TOG)* 41, 4 (2022), 1–15.
- [66] Johannes L Schonberger and Jan-Michael Frahm. 2016. Structure-from-motion revisited. In *Proceedings of the IEEE conference on computer vision and pattern recognition*. 4104–4113.
- [67] Bernhard Kerbl, Georgios Kopanas, Thomas Leimkühler, and George Drettakis. 2023. 3d gaussian splatting for real-time radiance field rendering. *ACM Trans. Graph.* 42, 4 (2023), 139–1.
- [68] Jiaxiang Tang, Jiawei Ren, Hang Zhou, Ziwei Liu, and Gang Zeng. 2023. Dreamgaussian: Generative gaussian splatting for efficient 3d content creation. *arXiv preprint arXiv:2309.16653* (2023).
- [69] Taoran Yi, Jiemin Fang, Junjie Wang, Guanjun Wu, Lingxi Xie, Xiaopeng Zhang, Wenyu Liu, Qi Tian, and Xinggang Wang. 2024. Gaussiandreamer: Fast generation from text to 3d gaussians by bridging 2d and 3d diffusion models. In *Proceedings of the IEEE/CVF Conference on Computer Vision and Pattern Recognition*. 6796–6807.
- [70] Wenrui Li, Fucheng Cai, Yapeng Mi, Zhe Yang, Wangmeng Zuo, Xingtao Wang, and Xiaopeng Fan. 2024. Scenedreamer360: Text-driven 3d-consistent scene generation with panoramic gaussian splatting. *arXiv preprint arXiv:2408.13711* (2024).
- [71] Eric R Chan, Connor Z Lin, Matthew A Chan, Koki Nagano, Boxiao Pan, Shalini De Mello, Orazio Gallo, Leonidas J Guibas, Jonathan Tremblay, Sameh Khamis, et al. 2022. Efficient geometry-aware 3d generative adversarial networks. In *Proceedings of the IEEE/CVF conference on computer vision and pattern recognition*. 16123–16133.
- [72] Tero Karras, Samuli Laine, Miika Aittala, Janne Hellsten, Jaakko Lehtinen, and Timo Aila. 2020. Analyzing and improving the image quality of stylegan. In *Proceedings of the IEEE/CVF conference on computer vision and pattern recognition*. 8110–8119.
- [73] Anpei Chen, Zexiang Xu, Andreas Geiger, Jingyi Yu, and Hao Su. 2022. Tensorf: Tensorial radiance fields. In *European conference on computer vision*. Springer, 333–350.
- [74] Tianchang Shen, Jun Gao, Kangxue Yin, Ming-Yu Liu, and Sanja Fidler. 2021. Deep marching tetrahedra: a hybrid representation for high-resolution 3d shape synthesis. *Advances in Neural Information Processing Systems* 34 (2021), 6087–6101.
- [75] Laura Downs, Anthony Francis, Nate Koenig, Brandon Kinman, Ryan Hickman, Krista Reymann, Thomas B McHugh, and Vincent Vanhoucke. 2022. Google scanned objects: A high-quality dataset of 3d scanned household items. In *2022 International Conference on Robotics and Automation (ICRA)*. IEEE, 2553–2560.
- [76] Xiaoxiao Long, Yuan-Chen Guo, Cheng Lin, Yuan Liu, Zhiyang Dou, Lingjie Liu, Yuexin Ma, Song-Hai Zhang, Marc Habermann, Christian Theobalt, et al. 2024. Wonder3d: Single image to 3d using cross-domain diffusion. In *Proceedings of the IEEE/CVF conference on computer vision and pattern recognition*. 9970–9980.

- [77] Yinghao Xu, Hao Tan, Fujun Luan, Sai Bi, Peng Wang, Jiahao Li, Zifan Shi, Kalyan Sunkavalli, Gordon Wetzstein, Zexiang Xu, et al. 2023. Dmv3d: Denoising multi-view diffusion using 3d large reconstruction model. *arXiv preprint arXiv:2311.09217* (2023).
- [78] Kailu Wu, Fangfu Liu, Zhihan Cai, Runjie Yan, Hanyang Wang, Yating Hu, Yueqi Duan, and Kaisheng Ma. 2024. Unique3d: High-quality and efficient 3d mesh generation from a single image. In *The Thirty-eighth Annual Conference on Neural Information Processing Systems*.
- [79] Thomas W Mitchel, Carlos Esteves, and Ameesh Makadia. 2024. Single mesh diffusion models with field latents for texture generation. In *Proceedings of the IEEE/CVF Conference on Computer Vision and Pattern Recognition*. 7953–7963.
- [80] Angel X Chang, Thomas Funkhouser, Leonidas Guibas, Pat Hanrahan, Qixing Huang, Zimo Li, Silvio Savarese, Manolis Savva, Shuran Song, Hao Su, et al. 2015. Shapenet: An information-rich 3d model repository. *arXiv preprint arXiv:1512.03012* (2015).
- [81] Tianyu Huang, Yihan Zeng, Bowen Dong, Hang Xu, Songcen Xu, Rynson WH Lau, and Wangmeng Zuo. 2023. Textfield3d: Towards enhancing open-vocabulary 3d generation with noisy text fields. *arXiv preprint arXiv:2309.17175* (2023).
- [82] Aditya Sanghi, Rao Fu, Vivian Liu, Karl DD Willis, Hooman Shayani, Amir H Khasahmadi, Srinath Sridhar, and Daniel Ritchie. 2023. Clip-sculptor: Zero-shot generation of high-fidelity and diverse shapes from natural language. In *Proceedings of the IEEE/CVF Conference on Computer Vision and Pattern Recognition*. 18339–18348.
- [83] Jiale Xu, Xintao Wang, Weihao Cheng, Yan-Pei Cao, Ying Shan, Xiaohu Qie, and Shenghua Gao. 2023. Dream3d: Zero-shot text-to-3d synthesis using 3d shape prior and text-to-image diffusion models. In *Proceedings of the IEEE/CVF Conference on Computer Vision and Pattern Recognition*. 20908–20918.
- [84] Zibo Zhao, Wen Liu, Xin Chen, Xianfang Zeng, Rui Wang, Pei Cheng, Bin Fu, Tao Chen, Gang Yu, and Shenghua Gao. 2023. Michelangelo: Conditional 3d shape generation based on shape-image-text aligned latent representation. *Advances in neural information processing systems* 36 (2023), 73969–73982.
- [85] Charlie Nash, Yaroslav Ganin, SM Ali Eslami, and Peter Battaglia. 2020. Polygen: An autoregressive generative model of 3d meshes. In *International conference on machine learning*. PMLR, 7220–7229.
- [86] Xingguang Yan, Liqiang Lin, Niloy J Mitra, Dani Lischinski, Daniel Cohen-Or, and Hui Huang. 2022. Shapeformer: Transformer-based shape completion via sparse representation. In *Proceedings of the IEEE/CVF Conference on Computer Vision and Pattern Recognition*. 6239–6249.
- [87] Linqi Zhou, Yilun Du, and Jiajun Wu. 2021. 3d shape generation and completion through point-voxel diffusion. In *Proceedings of the IEEE/CVF international conference on computer vision*. 5826–5835.
- [88] Dave Zhenyu Chen, Yawar Siddiqui, Hsin-Ying Lee, Sergey Tulyakov, and Matthias Nießner. 2023. Text2tex: Text-driven texture synthesis via diffusion models. In *Proceedings of the IEEE/CVF international conference on computer vision*. 18558–18568.
- [89] Zhirong Wu, Shuran Song, Aditya Khosla, Fisher Yu, Linguang Zhang, Xiaoou Tang, and Jianxiong Xiao. 2015. 3d shapenets: A deep representation for volumetric shapes. In *Proceedings of the IEEE conference on computer vision and pattern recognition*. 1912–1920.
- [90] Kaichun Mo, Shilin Zhu, Angel X Chang, Li Yi, Subarna Tripathi, Leonidas J Guibas, and Hao Su. 2019. Partnet: A large-scale benchmark for fine-grained and hierarchical part-level 3d object understanding. In *Proceedings of the IEEE/CVF conference on computer vision and pattern recognition*. 909–918.
- [91] Matt Deitke, Dustin Schwenk, Jordi Salvador, Luca Weihs, Oscar Michel, Eli VanderBilt, Ludwig Schmidt, Kiana Ehsani, Aniruddha Kembhavi, and Ali Farhadi. 2023. Objaverse: A universe of annotated 3d objects. In *Proceedings of the IEEE/CVF conference on computer vision and pattern recognition*. 13142–13153.
- [92] Zhaoxi Chen, Jiaxiang Tang, Yuhao Dong, Ziang Cao, Fangzhou Hong, Yushi Lan, Tengfei Wang, Haozhe Xie, Tong Wu, Shunsuke Saito, et al. 2024. 3dtopia-xl: Scaling high-quality 3d asset generation via primitive diffusion. *arXiv preprint arXiv:2409.12957* (2024).
- [93] Yichun Shi, Peng Wang, Jianglong Ye, Mai Long, Kejie Li, and Xiao Yang. 2023. Mvdream: Multi-view diffusion for 3d generation. *arXiv preprint arXiv:2308.16512* (2023).
- [94] Ruoshi Liu, Rundi Wu, Basile Van Hoorick, Pavel Tokmakov, Sergey Zakharov, and Carl Vondrick. 2023. Zero-1-to-3: Zero-shot one image to 3d object. In *Proceedings of the IEEE/CVF international conference on computer vision*. 9298–9309.
- [95] Ruoxi Shi, Hansheng Chen, Zhuoyang Zhang, Minghua Liu, Chao Xu, Xinyue Wei, Linghao Chen, Chong Zeng, and Hao Su. 2023. Zero123++: a single image to consistent multi-view diffusion base model. *arXiv preprint arXiv:2310.15110* (2023).
- [96] Zexiang Liu, Yangguang Li, Youtian Lin, Xin Yu, Sida Peng, Yan-Pei Cao, Xiaojuan Qi, Xiaoshui Huang, Ding Liang, and Wanli Ouyang. 2024. Unidream: Unifying diffusion priors for relightable text-to-3d generation. In *European Conference on Computer Vision*. Springer, 74–91.

- [97] Shitao Tang, Jiacheng Chen, Dilin Wang, Chengzhou Tang, Fuyang Zhang, Yuchen Fan, Vikas Chandra, Yasutaka Furukawa, and Rakesh Ranjan. 2024. Mvdiffusion++: A dense high-resolution multi-view diffusion model for single or sparse-view 3d object reconstruction. In *European Conference on Computer Vision*. Springer, 175–191.
- [98] Dong Huo, Zixin Guo, Xinxin Zuo, Zhihao Shi, Juwei Lu, Peng Dai, Songcen Xu, Li Cheng, and Yee-Hong Yang. 2024. Texgen: Text-guided 3d texture generation with multi-view sampling and resampling. In *European Conference on Computer Vision*. Springer, 352–368.
- [99] Xianfang Zeng, Xin Chen, Zhongqi Qi, Wen Liu, Zibo Zhao, Zhibin Wang, Bin Fu, Yong Liu, and Gang Yu. 2024. Paint3d: Paint anything 3d with lighting-less texture diffusion models. In *Proceedings of the IEEE/CVF conference on computer vision and pattern recognition*. 4252–4262.
- [100] Kim Youwang, Tae-Hyun Oh, and Gerard Pons-Moll. 2024. Paint-it: Text-to-texture synthesis via deep convolutional texture map optimization and physically-based rendering. In *Proceedings of the IEEE/CVF Conference on Computer Vision and Pattern Recognition*. 4347–4356.
- [101] Xin Huang, Tengfei Wang, Ziwei Liu, and Qing Wang. 2024. Material Anything: Generating Materials for Any 3D Object via Diffusion. *arXiv preprint arXiv:2411.15138* (2024).
- [102] Matt Deitke, Ruoshi Liu, Matthew Wallingford, Huong Ngo, Oscar Michel, Aditya Kusupati, Alan Fan, Christian Laforte, Vikram Voleti, Samir Yitzhak Gadre, et al. 2023. Objaverse-xl: A universe of 10m+ 3d objects. *Advances in Neural Information Processing Systems* 36 (2023), 35799–35813.
- [103] Jianfeng Xiang, Zelong Lv, Sicheng Xu, Yu Deng, Ruicheng Wang, Bowen Zhang, Dong Chen, Xin Tong, and Jiaolong Yang. 2024. Structured 3d latents for scalable and versatile 3d generation. *arXiv preprint arXiv:2412.01506* (2024).
- [104] Huan Fu, Rongfei Jia, Lin Gao, Mingming Gong, Binqiang Zhao, Steve Maybank, and Dacheng Tao. 2021. 3d-future: 3d furniture shape with texture. *International Journal of Computer Vision* 129 (2021), 3313–3337.
- [105] Yiqun Zhao, Zibo Zhao, Jing Li, Sixun Dong, and Shenghua Gao. 2024. RoomDesigner: Encoding anchor-latents for style-consistent and shape-compatible indoor scene generation. In *2024 International Conference on 3D Vision (3DV)*. IEEE, 1413–1423.
- [106] Jiapeng Tang, Yinyu Nie, Lev Markhasin, Angela Dai, Justus Thies, and Matthias Nießner. 2024. Diffuscene: Denoising diffusion models for generative indoor scene synthesis. In *Proceedings of the IEEE/CVF conference on computer vision and pattern recognition*. 20507–20518.
- [107] Zhennan Wu, Yang Li, Han Yan, Taizhang Shang, Weixuan Sun, Senbo Wang, Ruikai Cui, Weizhe Liu, Hiroyuki Sato, Hongdong Li, et al. 2024. Blockfusion: Expandable 3d scene generation using latent tri-plane extrapolation. *ACM Transactions on Graphics (TOG)* 43, 4 (2024), 1–17.
- [108] Huan Fu, Bowen Cai, Lin Gao, Ling-Xiao Zhang, Jiaming Wang, Cao Li, Qixun Zeng, Chengyue Sun, Rongfei Jia, Binqiang Zhao, et al. 2021. 3d-front: 3d furnished rooms with layouts and semantics. In *Proceedings of the IEEE/CVF International Conference on Computer Vision*. 10933–10942.
- [109] Yandan Yang, Baoxiong Jia, Peiyuan Zhi, and Siyuan Huang. 2024. Physcene: Physically interactable 3d scene synthesis for embodied ai. In *Proceedings of the IEEE/CVF Conference on Computer Vision and Pattern Recognition*. 16262–16272.
- [110] Qihang Zhang, Yinghao Xu, Yujun Shen, Bo Dai, Bolei Zhou, and Ceyuan Yang. 2024. Berfscene: Bev-conditioned equivariant radiance fields for infinite 3d scene generation. In *Proceedings of the IEEE/CVF Conference on Computer Vision and Pattern Recognition*. 6839–6849.
- [111] Yinghao Xu, Menglei Chai, Zifan Shi, Sida Peng, Ivan Skorokhodov, Aliaksandr Siarohin, Ceyuan Yang, Yujun Shen, Hsin-Ying Lee, Bolei Zhou, et al. 2023. Discoscene: Spatially disentangled generative radiance fields for controllable 3d-aware scene synthesis. In *Proceedings of the IEEE/CVF conference on computer vision and pattern recognition*. 4402–4412.
- [112] Guangyao Zhai, Evin Pınar Örnek, Shun-Cheng Wu, Yan Di, Federico Tombari, Nassir Navab, and Benjamin Busam. 2023. Commonsences: Generating commonsense 3d indoor scenes with scene graph diffusion. *Advances in Neural Information Processing Systems* 36 (2023), 30026–30038.
- [113] Dave Zhenyu Chen, Haoxuan Li, Hsin-Ying Lee, Sergey Tulyakov, and Matthias Nießner. 2024. Scenetex: High-quality texture synthesis for indoor scenes via diffusion priors. In *Proceedings of the IEEE/CVF Conference on Computer Vision and Pattern Recognition*. 21081–21091.
- [114] Quan Meng, Lei Li, Matthias Nießner, and Angela Dai. 2024. Lt3sd: Latent trees for 3d scene diffusion. *arXiv preprint arXiv:2409.08215* (2024).
- [115] Xianggang Yu, Mutian Xu, Yidan Zhang, Haolin Liu, Chongjie Ye, Yushuang Wu, Zizheng Yan, Chenming Zhu, Zhangyang Xiong, Tianyou Liang, et al. 2023. Mvimgnet: A large-scale dataset of multi-view images. In *Proceedings of the IEEE/CVF conference on computer vision and pattern recognition*. 9150–9161.
- [116] Angela Dai, Angel X Chang, Manolis Savva, Maciej Halber, Thomas Funkhouser, and Matthias Nießner. 2017. Scannet: Richly-annotated 3d reconstructions of indoor scenes. In *Proceedings of the IEEE conference on computer vision and pattern recognition*. 5828–5839.

- [117] Lukas Höllein, Ang Cao, Andrew Owens, Justin Johnson, and Matthias Nießner. 2023. Text2room: Extracting textured 3d meshes from 2d text-to-image models. In *Proceedings of the IEEE/CVF International Conference on Computer Vision*. 7909–7920.
- [118] Mike Roberts, Jason Ramapuram, Anurag Ranjan, Atulit Kumar, Miguel Angel Bautista, Nathan Paczan, Russ Webb, and Joshua M Susskind. 2021. Hypersim: A photorealistic synthetic dataset for holistic indoor scene understanding. In *Proceedings of the IEEE/CVF international conference on computer vision*. 10912–10922.
- [119] Jonas Schult, Sam Tsai, Lukas Höllein, Bichen Wu, Jialiang Wang, Chih-Yao Ma, Kunpeng Li, Xiaofang Wang, Felix Wimbauer, Zijian He, et al. 2024. Controlroom3d: Room generation using semantic proxy rooms. In *Proceedings of the IEEE/CVF Conference on Computer Vision and Pattern Recognition*. 6201–6210.
- [120] Jeremy Reizenstein, Roman Shapovalov, Philipp Henzler, Luca Sbordon, Patrick Labatut, and David Novotny. 2021. Common objects in 3d: Large-scale learning and evaluation of real-life 3d category reconstruction. In *Proceedings of the IEEE/CVF international conference on computer vision*. 10901–10911.
- [121] Luke Melas-Kyriazi, Iro Laina, Christian Rupprecht, and Andrea Vedaldi. 2023. Realfusion: 360deg reconstruction of any object from a single image. In *Proceedings of the IEEE/CVF conference on computer vision and pattern recognition*. 8446–8455.
- [122] Xingchen Liu, Piyush Tayal, Jianyuan Wang, Jesus Zarzar, Tom Monnier, Konstantinos Tertikas, Jiali Duan, Antoine Toisoul, Jason Y Zhang, Natalia Neverova, et al. 2025. UnCommon Objects in 3D. *arXiv preprint arXiv:2501.07574* (2025).
- [123] Kevin Chen, Christopher B Choy, Manolis Savva, Angel X Chang, Thomas Funkhouser, and Silvio Savarese. 2019. Text2shape: Generating shapes from natural language by learning joint embeddings. In *Computer Vision—ACCV 2018: 14th Asian Conference on Computer Vision, Perth, Australia, December 2–6, 2018, Revised Selected Papers, Part III 14*. Springer, 100–116.
- [124] Rao Fu, Xiao Zhan, Yiwen Chen, Daniel Ritchie, and Srinath Sridhar. 2022. Shapecrafter: A recursive text-conditioned 3d shape generation model. *Advances in Neural Information Processing Systems* 35 (2022), 8882–8895.
- [125] Alec Radford, Jong Wook Kim, Chris Hallacy, Aditya Ramesh, Gabriel Goh, Sandhini Agarwal, Girish Sastry, Amanda Askell, Pamela Mishkin, Jack Clark, et al. 2021. Learning transferable visual models from natural language supervision. In *International conference on machine learning*. PmlR, 8748–8763.
- [126] Can Wang, Menglei Chai, Mingming He, Dongdong Chen, and Jing Liao. 2022. Clip-nerf: Text-and-image driven manipulation of neural radiance fields. In *Proceedings of the IEEE/CVF conference on computer vision and pattern recognition*. 3835–3844.
- [127] Nasir Mohammad Khalid, Tianhao Xie, Eugene Belilovsky, and Tiberiu Popa. 2022. Clip-mesh: Generating textured meshes from text using pretrained image-text models. In *SIGGRAPH Asia 2022 conference papers*. 1–8.
- [128] Oscar Michel, Roi Bar-On, Richard Liu, Sagie Benaim, and Rana Hanocka. 2022. Text2mesh: Text-driven neural stylization for meshes. In *Proceedings of the IEEE/CVF conference on computer vision and pattern recognition*. 13492–13502.
- [129] Robin Rombach, Andreas Blattmann, Dominik Lorenz, Patrick Esser, and Björn Ommer. 2022. High-resolution image synthesis with latent diffusion models. In *Proceedings of the IEEE/CVF conference on computer vision and pattern recognition*. 10684–10695.
- [130] Jiahao Ge, Mingjun Zhou, Wenrui Bao, Hao Xu, and Chi-Wing Fu. 2024. Creating LEGO Figurines from Single Images. *ACM Transactions on Graphics (TOG)* 43, 4 (2024), 1–16.
- [131] Diederik P Kingma, Max Welling, et al. 2013. Auto-encoding variational bayes.
- [132] Lin Gao, Tong Wu, Yu-Jie Yuan, Ming-Xian Lin, Yu-Kun Lai, and Hao Zhang. 2021. Tm-net: Deep generative networks for textured meshes. *ACM Transactions on Graphics (TOG)* 40, 6 (2021), 1–15.
- [133] Ian Goodfellow, Jean Pouget-Abadie, Mehdi Mirza, Bing Xu, David Warde-Farley, Sherjil Ozair, Aaron Courville, and Yoshua Bengio. 2014. Generative adversarial nets. *Advances in neural information processing systems* 27 (2014).
- [134] Thu Nguyen-Phuoc, Chuan Li, Lucas Theis, Christian Richardt, and Yong-Liang Yang. 2019. Hologan: Unsupervised learning of 3d representations from natural images. In *Proceedings of the IEEE/CVF international conference on computer vision*. 7588–7597.
- [135] Thu H Nguyen-Phuoc, Christian Richardt, Long Mai, Yongliang Yang, and Niloy Mitra. 2020. Blockgan: Learning 3d object-aware scene representations from unlabelled images. *Advances in neural information processing systems* 33 (2020), 6767–6778.
- [136] Philipp Henzler, Niloy J Mitra, and Tobias Ritschel. 2019. Escaping plato’s cave: 3d shape from adversarial rendering. In *Proceedings of the IEEE/CVF International Conference on Computer Vision*. 9984–9993.
- [137] Aäron Van Den Oord, Nal Kalchbrenner, and Koray Kavukcuoglu. 2016. Pixel recurrent neural networks. In *International conference on machine learning*. PMLR, 1747–1756.
- [138] Alec Radford, Karthik Narasimhan, Tim Salimans, Ilya Sutskever, et al. 2018. Improving language understanding by generative pre-training. (2018).

- [139] Ashish Vaswani, Noam Shazeer, Niki Parmar, Jakob Uszkoreit, Llion Jones, Aidan N Gomez, Łukasz Kaiser, and Illia Polosukhin. 2017. Attention is all you need. *Advances in neural information processing systems* 30 (2017).
- [140] Jonathan Ho, Ajay Jain, and Pieter Abbeel. 2020. Denoising diffusion probabilistic models. *Advances in neural information processing systems* 33 (2020), 6840–6851.
- [141] Jascha Sohl-Dickstein, Eric Weiss, Niru Maheswaranathan, and Surya Ganguli. 2015. Deep unsupervised learning using nonequilibrium thermodynamics. In *International conference on machine learning*. pmlr, 2256–2265.
- [142] Junshu Tang, Tengfei Wang, Bo Zhang, Ting Zhang, Ran Yi, Lizhuang Ma, and Dong Chen. 2023. Make-it-3d: High-fidelity 3d creation from a single image with diffusion prior. In *Proceedings of the IEEE/CVF international conference on computer vision*. 22819–22829.
- [143] Yixun Liang, Xin Yang, Jiantao Lin, Haodong Li, Xiaogang Xu, and Yingcong Chen. 2024. Luciddreamer: Towards high-fidelity text-to-3d generation via interval score matching. In *Proceedings of the IEEE/CVF conference on computer vision and pattern recognition*. 6517–6526.
- [144] Taoran Yi, Jiemin Fang, Zanwei Zhou, Junjie Wang, Guanjun Wu, Lingxi Xie, Xiaopeng Zhang, Wenyu Liu, Xinggang Wang, and Qi Tian. 2024. Gaussiandreamerpro: Text to manipulable 3d gaussians with highly enhanced quality. *arXiv preprint arXiv:2406.18462* (2024).
- [145] Edward J Hu, Yelong Shen, Phillip Wallis, Zeyuan Allen-Zhu, Yuanzhi Li, Shean Wang, Lu Wang, Weizhu Chen, et al. 2022. Lora: Low-rank adaptation of large language models. *ICLR* 1, 2 (2022), 3.
- [146] Simo Ryu. 2023. Low-rank adaptation for fast text-to-image diffusion fine-tuning. *Low-rank adaptation for fast text-to-image diffusion fine-tuning* 3 (2023).
- [147] Baorui Ma, Haoge Deng, Junsheng Zhou, Yu-Shen Liu, Tiejun Huang, and Xinlong Wang. 2023. Geodream: Disentangling 2d and geometric priors for high-fidelity and consistent 3d generation. *arXiv preprint arXiv:2311.17971* (2023).
- [148] Yuan Liu, Cheng Lin, Zijiao Zeng, Xiaoxiao Long, Lingjie Liu, Taku Komura, and Wenping Wang. 2023. Syncdreamer: Generating multiview-consistent images from a single-view image. *arXiv preprint arXiv:2309.03453* (2023).
- [149] Yuan Li, Cheng Lin, Yuan Liu, Xiaoxiao Long, Chenxu Zhang, Ningna Wang, Xin Li, Wenping Wang, and Xiaohu Guo. 2025. CADDreamer: CAD object Generation from Single-view Images. *arXiv preprint arXiv:2502.20732* (2025).
- [150] Qiao Yu, Xianzhi Li, Yuan Tang, Xu Han, Long Hu, Yixue Hao, and Min Chen. 2024. Fancy123: One Image to High-Quality 3D Mesh Generation via Plug-and-Play Deformation. *arXiv preprint arXiv:2411.16185* (2024).
- [151] Minghao Chen, Roman Shapovalov, Iro Laina, Tom Monnier, Jianyuan Wang, David Novotny, and Andrea Vedaldi. 2024. PartGen: Part-level 3D Generation and Reconstruction with Multi-View Diffusion Models. *arXiv preprint arXiv:2412.18608* (2024).
- [152] Elad Richardson, Gal Metzger, Yuval Alaluf, Raja Giryes, and Daniel Cohen-Or. 2023. Texture: Text-guided texturing of 3d shapes. In *ACM SIGGRAPH 2023 conference proceedings*. 1–11.
- [153] Tianshi Cao, Karsten Kreis, Sanja Fidler, Nicholas Sharp, and Kangxue Yin. 2023. Textfusion: Synthesizing 3d textures with text-guided image diffusion models. In *Proceedings of the IEEE/CVF International Conference on Computer Vision*. 4169–4181.
- [154] Kai Wang, Manolis Savva, Angel X Chang, and Daniel Ritchie. 2018. Deep convolutional priors for indoor scene synthesis. *ACM Transactions on Graphics (TOG)* 37, 4 (2018), 1–14.
- [155] Zhaoxi Chen, Guangcong Wang, and Ziwei Liu. 2023. Scenedreamer: Unbounded 3d scene generation from 2d image collections. *IEEE transactions on pattern analysis and machine intelligence* 45, 12 (2023), 15562–15576.
- [156] Haozhe Xie, Zhaoxi Chen, Fangzhou Hong, and Ziwei Liu. 2024. Citydreamer: Compositional generative model of unbounded 3d cities. In *Proceedings of the IEEE/CVF conference on computer vision and pattern recognition*. 9666–9675.
- [157] Haozhe Xie, Zhaoxi Chen, Fangzhou Hong, and Ziwei Liu. 2024. GaussianCity: Generative Gaussian splatting for unbounded 3D city generation. *arXiv preprint arXiv:2406.06526* (2024).
- [158] Ryan Po and Gordon Wetzstein. 2024. Compositional 3d scene generation using locally conditioned diffusion. In *2024 International Conference on 3D Vision (3DV)*. IEEE, 651–663.
- [159] Dave Epstein, Ben Poole, Ben Mildenhall, Alexei A Efros, and Aleksander Holynski. 2024. Disentangled 3d scene generation with layout learning. *arXiv preprint arXiv:2402.16936* (2024).
- [160] Yongwei Chen, Tengfei Wang, Tong Wu, Xingang Pan, Kui Jia, and Ziwei Liu. 2024. Comboverse: Compositional 3d assets creation using spatially-aware diffusion guidance. In *European Conference on Computer Vision*. Springer, 128–146.
- [161] Zizheng Yan, Jiapeng Zhou, Fanpeng Meng, Yushuang Wu, Lingteng Qiu, Zisheng Ye, Shuguang Cui, Guanying Chen, and Xiaoguang Han. 2024. Dreamdissector: Learning disentangled text-to-3d generation from 2d diffusion priors. In *European Conference on Computer Vision*. Springer, 124–141.
- [162] Song-Hai Zhang, Shao-Kui Zhang, Wei-Yu Xie, Cheng-Yang Luo, Yong-Liang Yang, and Hongbo Fu. 2021. Fast 3D indoor scene synthesis by learning spatial relation priors of objects. *IEEE Transactions on Visualization and Computer Graphics* 28, 9 (2021), 3082–3092.

- [163] Guangyao Zhai, Evin Pınar Örnek, Dave Zhenyu Chen, Ruotong Liao, Yan Di, Nassir Navab, Federico Tombari, and Benjamin Busam. 2024. Echoscene: Indoor scene generation via information echo over scene graph diffusion. In *European Conference on Computer Vision*. Springer, 167–184.
- [164] Ziniu Hu, Ahmet Iscen, Aashi Jain, Thomas Kipf, Yisong Yue, David A Ross, Cordelia Schmid, and Alireza Fathi. 2024. Scenecraft: An llm agent for synthesizing 3d scenes as blender code. In *Forty-first International Conference on Machine Learning*.
- [165] Qixuan Li, Chao Wang, Zongjin He, and Yan Peng. 2025. PhiP-G: Physics-Guided Text-to-3D Compositional Scene Generation. *arXiv preprint arXiv:2502.00708* (2025).
- [166] Zifan Shi, Yujun Shen, Jiapeng Zhu, Dit-Yan Yeung, and Qifeng Chen. 2022. 3d-aware indoor scene synthesis with depth priors. In *European Conference on Computer Vision*. Springer, 406–422.
- [167] Miguel Angel Bautista, Pengsheng Guo, Samira Abnar, Walter Talbott, Alexander Toshev, Zhuoyuan Chen, Laurent Dinh, Shuangfei Zhai, Hanlin Goh, Daniel Ulbricht, et al. 2022. Gaudi: A neural architect for immersive 3d scene generation. *Advances in Neural Information Processing Systems* 35 (2022), 25102–25116.
- [168] Seung Wook Kim, Bradley Brown, Kangxue Yin, Karsten Kreis, Katja Schwarz, Daiqing Li, Robin Rombach, Antonio Torralba, and Sanja Fidler. 2023. Neuralfield-ldm: Scene generation with hierarchical latent diffusion models. In *Proceedings of the IEEE/CVF conference on computer vision and pattern recognition*. 8496–8506.
- [169] Jingbo Zhang, Xiaoyu Li, Ziyu Wan, Can Wang, and Jing Liao. 2024. Text2nerf: Text-driven 3d scene generation with neural radiance fields. *IEEE Transactions on Visualization and Computer Graphics* 30, 12 (2024), 7749–7762.
- [170] Liangchen Song, Liangliang Cao, Hongyu Xu, Kai Kang, Feng Tang, Junsong Yuan, and Yang Zhao. 2023. Roomdreamer: Text-driven 3d indoor scene synthesis with coherent geometry and texture. *arXiv preprint arXiv:2305.11337* (2023).
- [171] Shijie Zhou, Zhiwen Fan, Dejia Xu, Haoran Chang, Pradyumna Chari, Tejas Bharadwaj, Suya You, Zhangyang Wang, and Achuta Kadambi. 2024. Dreamscene360: Unconstrained text-to-3d scene generation with panoramic gaussian splatting. In *European Conference on Computer Vision*. Springer, 324–342.
- [172] Jianyi Wang, Kelvin CK Chan, and Chen Change Loy. 2023. Exploring clip for assessing the look and feel of images. In *Proceedings of the AAAI conference on artificial intelligence*, Vol. 37. 2555–2563.
- [173] Haoxi Ran, Vitor Guizilini, and Yue Wang. 2024. Towards realistic scene generation with lidar diffusion models. In *Proceedings of the IEEE/CVF Conference on Computer Vision and Pattern Recognition*. 14738–14748.
- [174] Markus Lipp, Daniel Scherzer, Peter Wonka, and Michael Wimmer. 2011. Interactive modeling of city layouts using layers of procedural content. In *Computer Graphics Forum*, Vol. 30. Wiley Online Library, 345–354.
- [175] Carlos A Vanegas, Tom Kelly, Basil Weber, Jan Halatsch, Daniel G Aliaga, and Pascal Müller. 2012. Procedural generation of parcels in urban modeling. In *Computer graphics forum*, Vol. 31. Wiley Online Library, 681–690.
- [176] Jerry O Talton, Yu Lou, Steve Lesser, Jared Duke, Radomir Mech, and Vladlen Koltun. 2011. Metropolis procedural modeling. *ACM Trans. Graph.* 30, 2 (2011), 11–1.
- [177] Paul Merrell. 2023. Example-based procedural modeling using graph grammars. *ACM Transactions on Graphics (TOG)* 42, 4 (2023), 1–16.
- [178] Blender Online Community. 2018. *Blender - a 3D modelling and rendering package*. Blender Foundation, Stichting Blender Foundation, Amsterdam. <http://www.blender.org>
- [179] Alexander Raistrick, Lingjie Mei, Karhan Kayan, David Yan, Yiming Zuo, Beining Han, Hongyu Wen, Meenal Parakh, Stamatis Alexandropoulos, Lahav Lipson, et al. 2024. Infinigen indoors: Photorealistic indoor scenes using procedural generation. In *Proceedings of the IEEE/CVF Conference on Computer Vision and Pattern Recognition*. 21783–21794.
- [180] Mengqi Zhou, Yuxi Wang, Jun Hou, Shougao Zhang, Yiwei Li, Chuanchen Luo, Junran Peng, and Zhaoxiang Zhang. 2024. SceneX: Procedural Controllable Large-scale Scene Generation. *arXiv preprint arXiv:2403.15698* (2024).
- [181] Shougao Zhang, Mengqi Zhou, Yuxi Wang, Chuanchen Luo, Rongyu Wang, Yiwei Li, Zhaoxiang Zhang, and Junran Peng. 2024. Cityx: Controllable procedural content generation for unbounded 3d cities. *arXiv preprint arXiv:2407.17572* (2024).
- [182] Esri. 2024. *CityEngine*. <https://www.esri.com/en-us/arcgis/products/arcgis-cityengine/overview>
- [183] Yuze He, Yushi Bai, Matthieu Lin, Wang Zhao, Yubin Hu, Jenny Sheng, Ran Yi, Juanzi Li, and Yong-Jin Liu. 2023. T³Bench: Benchmarking Current Progress in Text-to-3D Generation. arXiv:2310.02977 [cs.CV]
- [184] Jack Hessel, Ari Holtzman, Maxwell Forbes, Ronan Le Bras, and Yejin Choi. 2021. Clipscore: A reference-free evaluation metric for image captioning. *arXiv preprint arXiv:2104.08718* (2021).
- [185] Boyuan Chen, Hanxiao Jiang, Shaowei Liu, Saurabh Gupta, Yunzhu Li, Hao Zhao, and Shenlong Wang. 2025. Phys-Gen3D: Crafting a Miniature Interactive World from a Single Image. *arXiv preprint arXiv:2503.20746* (2025).
- [186] Qiyu Dai, Xingyu Ni, Qianfan Shen, Wenzheng Chen, Baoquan Chen, and Mengyu Chu. 2025. RainyGS: Efficient Rain Synthesis with Physically-Based Gaussian Splatting. *arXiv preprint arXiv:2503.21442* (2025).
- [187] Yuheng Liu, Xinke Li, Xueting Li, Lu Qi, Chongshou Li, and Ming-Hsuan Yang. 2024. Pyramid diffusion for fine 3d large scene generation. In *European Conference on Computer Vision*. Springer, 71–87.

A TIMELINE OF 3D OBJECT GENERATION METHODS

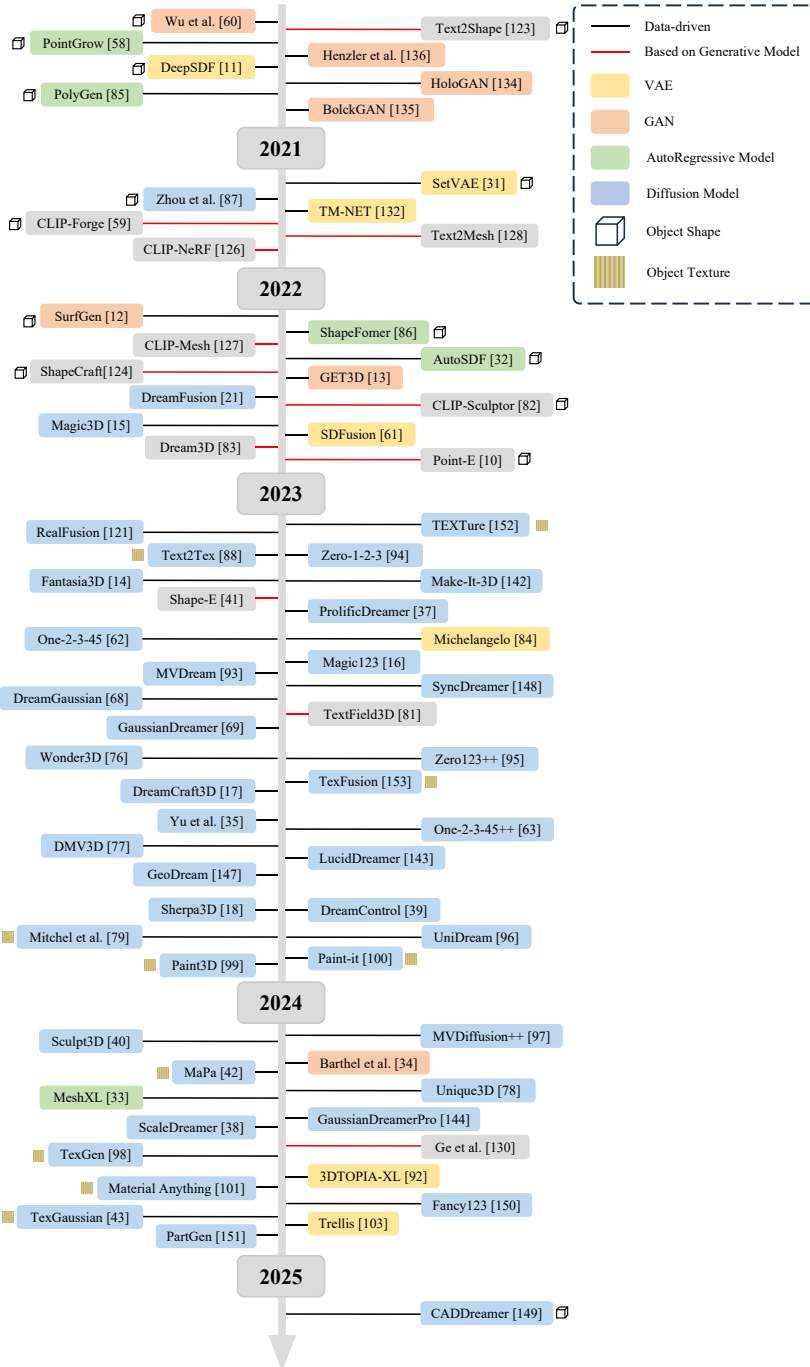


Fig. 5. Timeline of 3D Object Generation Methods. If a approach is accompanied by an icon, it indicates that the method focuses on generating object shape or textures. Otherwise, it addresses both aspects simultaneously.

B TIMELINE OF 3D SCENE GENERATION METHODS

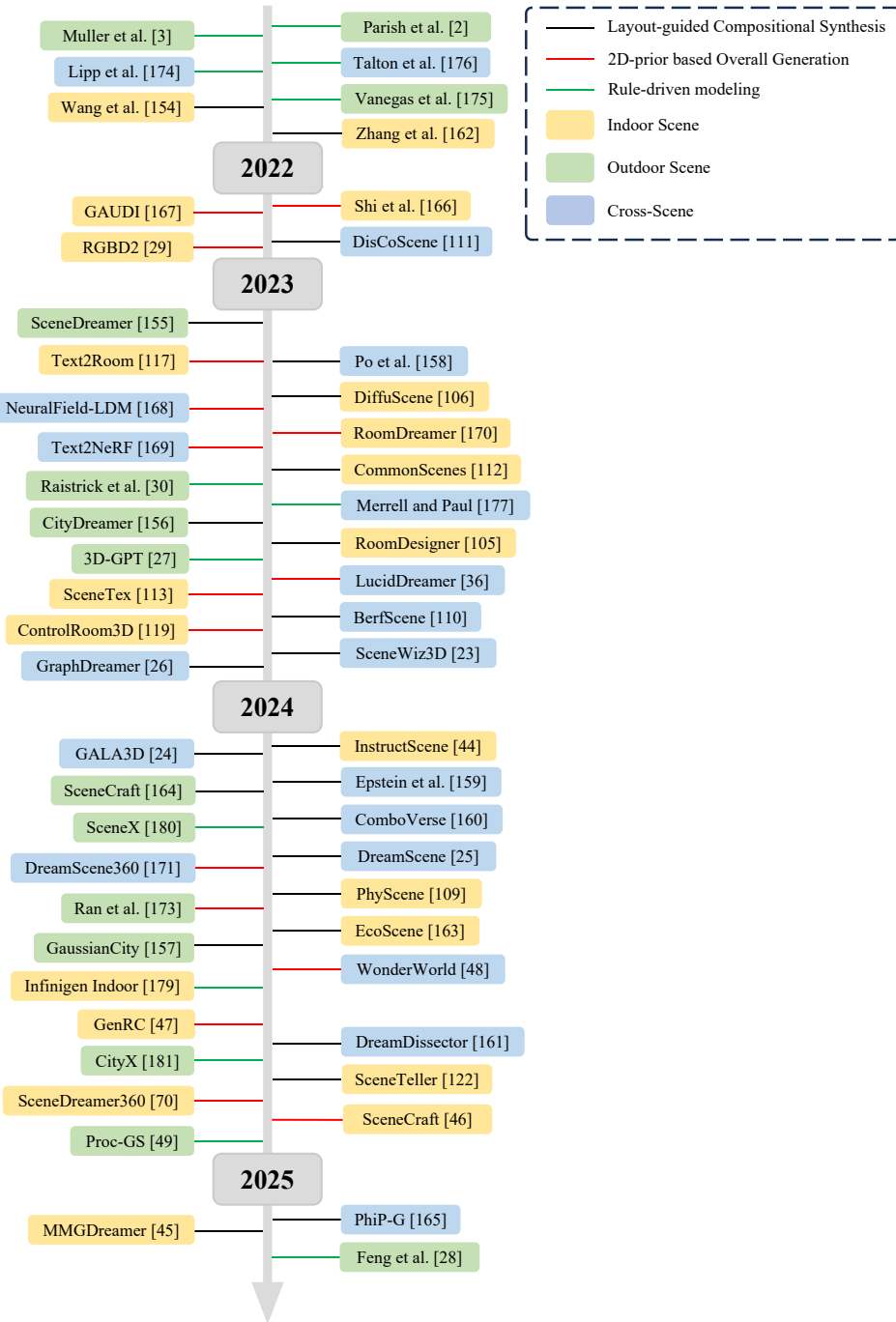


Fig. 6. Timeline of 3D Scene Generation Methods.